JOURNAL INTERNATIONAL D'ACOUSTIQUE
sous le patronage
du Groupement des Acousticiens
de Langue Française

INTERNATIONAL JOURNAL ON ACOUSTICS
sponsored by the Acoustics Group
of the Physical Society
of London

INTERNATIONALE AKUSTISCHE ZEITSCHRIFT
Unter Mitwirkung
des Verbandes der Deutschen
Physikalischen Gesellschaften

ACUSTICA

edited by
Prof. Dr. C. W. KOSTEN
editor-in-chief
DELFT

publié par
Dr. F. CANAC
MARSEILLE

Dr. E. G. RICHARDSON
NEWCASTLE UPON TYNE

herausgegeben von
Prof. Dr. E. MEYER
GOTTINGEN

Prof. Dr. A. GIACOMINI
ROMA

TABLE DE MATIÈRES — CONTENTS — INHALT

LEHR, The system of the Hemony-carillons tuning . . . . *101—104*
MERLE, Emploi des ondes ultrasonores pour l'étude d'un champ aérodynamique . *104—108*
AYERS and MORTON, The subjective calibration of bone-conduction receivers for hearing aids . . . . *109—113*
SMITS and KOSTEN, Sound absorption by slit resonators . . . . *114—122*
KING and MAGUIRE, The pressure and field calibration of microphones . . . . *123—130*
MEYER und KARMANN, Die Schwingung der Luftteilchen in der Nähe einer schallabsorbierenden Wand . . . . *130—136*
FERRERO and SACERDOTE, Parameters of sound propagation in granular absorbent materials . . . . *137—142*

S. HIRZEL VERLAG · ZÜRICH

Vol. 1, No. 3 — 1951 — pp. 101—144

Reprinted with the permission of S. Hirzel Verlag, Stuttgart

JOHNSON REPRINT CORPORATION
111 Fifth Avenue, New York, N.Y. 10003

JOHNSON REPRINT COMPANY LIMITED
Berkeley Square House, London, W.1

First reprinting, 1967, Johnson Reprint Corporation

Printed in the United States of America

ACUSTICA

VOL. 1 1951 No. 3

THE SYSTEM OF THE HEMONY-CARILLONS TUNING

by ANDRÉ LEHR

Netherlands Bellfoundry "Eijsbouts-Lips" Ltd., Asten, Holland

Summary

A tone-recording of three HEMONY carillons (namely: Delft, Kampen and Middelstum) has been made with electronic measuring instruments. The object was to find out which sort of tuning the HEMONYS used. The results show that the HEMONYS used meantone tuning.

Sommaire

On a enregistré électroniquement la tonalité de trois carillons HEMONY (à savoir: ceux de Delft, Kampen et Middelstum). Il s'agissait de déterminer quel tempérament a été utilisé. Les résultats montrent que c'est celui du son moyen.

Zusammenfassung

Mit elektrischen Meßinstrumenten wurde eine Klangaufnahme von drei HEMONY-Glockenspielen (nämlich Delft, Kampen und Middelstum) gemacht, mit dem Ziel herauszufinden, welche Stimmung die HEMONYS benutzten. Die Ergebnisse zeigten, daß die HEMONYS die Mitteltonstimmung benutzten.

1. Introduction

The carillons of François and Pierre HEMONY which are so often found in the Netherlands have always been a point of interest to historians, bell-experts and acoustic-scientists. In spite of this the problem has never been considered: what type of tuning the bros. HEMONY used, just-tempered, meantone or another sort of tuning? It is generally assumed that their carillons were mostly under just-tempered tuning. Strange, for during the 17th century meantone tuning was often applied. For correct investigation of this matter it was necessary to make an accurate tone recording of HEMONY carillons.

This has lately been done by the Nederlandse Klokkengieterij Eijsbouts-Lips, Asten, Holland to three carillons, namely Delft, Kampen and Middelstum, using electronic measuring instruments. The note diagrams Figs. 1 and 2 give the HEMONY-bell-recordings of Kampen and Delft. Bells which have been cast later are not quoted here. On the lower side of the horizontal axis the semitones are given corresponding with the equitempered tuning taking the base as $a' = 435$. On the vertical axis the deviation for the hum note (large circles), prime (small circles) and octave (dots) (the three important partials of the bell) is stated in "cents". An accurately tuned bell is thus one for which the large circle, the small circle and the dot coincide. This is for example the case for the f′ and a′ of the Kampen carillon. If the mutual deviation is not larger than 10 cents i. e. the circles in the graph are still in contact, we can still talk about a well-tuned bell. This is usually the case. On the upper side of the horizontal axis (top of Fig.), the notes are stated as they appear on the keyboard. In the Delft carillon cis-28 cents is labelled c (Fig. 1). This is normal for the HEMONY's; they tuned higher than $a' = 435$. In the Kampen carillon gis-14 cents is called c (Fig. 2). Gis-14 cents is the normal g of HEMONY. Since it is called c the carillon is said to be transposed from g to c. Transposition is common practice for economical reasons since in that way the total mass, and therefore the cost of the carillon, is reduced. Considering the graphs carefully, the first thing we notice is that the semitones are not the same, for, then, all the bells would lie on a horizontal line. In what system of tuning are these bells made then? Firstly we must state the exact pitch of the sound. It is known now that the pitch of the bell is defined by the striking note.

It gives us the first impression of the tone-quality but can only be heard for a very short time. The octave of a well-tuned bell is always a clear octave higher than the striking note, and, since the octave can be heard much longer than the striking

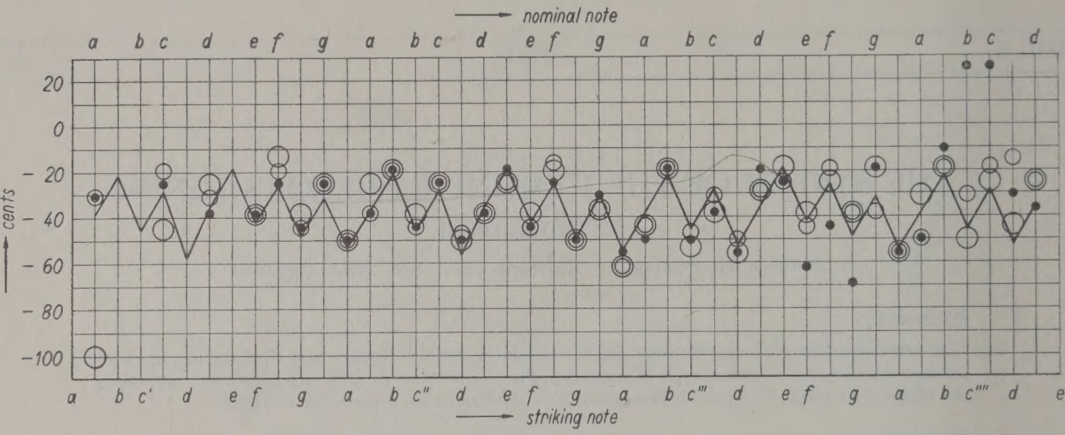

Fig. 1. Carillon Delft.

note, the octave is a very suitable partial for measuring the pitch of a bell. The pitch will be defined, therefore, as one octave below the partial called "octave". The prime is less suitable to serve our purpose since only in bells with an extreme preciseness of tuning is the striking note of the same pitch as the prime.

2. The Delft carillon

As Fig. 1 shows us, this carillon belongs to one of the superior categories. François Hemony founded and tuned it in 1661. Practically for all the bells, the hum note, prime and octave lie within the limited tolerance.

Only the smallest bells show clear deviations in the octaves originating in the difficulties, which Hemony had while tuning these small carillon-bells. It is advisable to omit the highest octave from our investigations, noting only the bells from cis′ till cis‴. The octaves which are proportional to the striking note are given in Table I, second and third column. Errors that have inevitably been made at the tuning and the tone-recording are reduced by averaging these two octaves (fourth column). Applying the just tempered tuning system, it is clearly shown that the carillon is indeed not just tempered, for the second should be 204, the minor third 316 cents higher than the prime. From the table we see that this is definitely not the case. Let us now try meantone tuning. This means that the fifths from F till a′ are reduced to such a state, that f′—a′ form a clear third; so the fifths only become 5 cents too small. For the greater part the third remains just tempered. In Table II the intervals of the meantone tuning are indicated as deviations (in cents) in relation to the equi-tempered tuning. Comparing the average recording of the Delft carillon (Table I, 4) with the meantone tuning, beginning at cis-25 cents (Table I, 5) it is obvious that we can surely regard this carillon as made in this system of tuning. It is not absolutely positive however that the base is cis-25 cents, for we have to consider an average, i. e. the number 25 should be adopted so as to make the sum of the deviations between column 4 ("average") and column 5 ("mean-

Table I

Carillon Delft

Interval	cis′-cis″	cis″-cis‴	average	meantone tuning base cis-25	meantone tuning base cis-28
prime	— 25	— 25	— 25	— 25	— 28
semitone		— 50	— 50	— 49	— 52
second	— 38	— 38	— 38	— 32	— 35
minor third		— 19	— 19	— 15	— 18
third	— 38	— 44	— 41	— 39	— 42
fourth	— 25	— 25	— 25	— 22	— 25
augm. fourth . . .	— 44	— 50	— 47	— 45	— 48
fifth	— 25	— 31	— 28	— 28	— 31
augm. fifth	— 50	— 56	— 53	— 52	— 55
sixth	— 38	— 50	— 44	— 35	— 38
dimin. seventh . .	— 19	— 19	— 19	— 18	— 21
seventh	— 44	— 50	— 47	— 42	— 45

Table II

The meantone tuning compared with the equi-tempered tuning

Interval	Deviations in cents
prime	0
semitone	— 24
second	— 7
minor third	+ 10
third	— 14
fourth	+ 3
augm. fourth . .	— 20
fifth	— 3
augm. fifth . . .	— 27
sixth	— 10
dimin. seventh .	+ 7
seventh	— 17

tone tuning") zero. Starting from this, we can calculate the correct base, only of course if we can assume that the above conclusion is correct. This base then must be cis-28 cents. From this we can again make a table (Table I, 6) that shows the arrangement of the bells after an accurate tuning by Hemony, still assuming that our theory is right. Comparing with the reality, the mean deviation seems to be ± 4 cents, including the errors made by Hemony, those made by us in recording the tone and later alterations in precision due to weather (erosion etc.). Bearing this in mind, ± 4 cents is practically negligible, so giving us reason to think that François Hemony has made the Delft carillon in meantone tuning. The drawn line in Fig. 1 gives this system of tuning as Table I, 6 does. Applying the above to the Kampen carillon, we get practically the same result.

3. The Kampen carillon

It would be useful to go through some of this carillon's history. Kampen, the town where the most well-known bellfounder prior to Hemony, Gerryt van Wou, lived and worked during the end of the 15th century, possessed various heavy bells made by the latter founder. François Hemony cast and tuned the carillon in 1659 and in 1662; van Wou's bells (gis, bes, c′ and g′) have been incorporated in the carillon. Naturally the pitch was not right, this is why Hemony tuned the bells. He did the same with the es′, cast by Wegewaert in 1627. The tuning did not turn out as he had expected it to, which can also be seen in Fig. 2. In the carillon however they are satisfactory, for the octaves (proportional to the striking note) are correct. The bell g‴ was recast later. Like the Delft carillon only the bells from gis till gis‴ are considered. From this, a corresponding table, III, can be formed. It is quite clear now that this carillon, which has an average base gis-14 cents, is made in the meantone tuning. The greatest deviation appears at the prime of the third octave, which is 11 cents too low. The average deviation is ± 5 cents, a factor which we can take to be correct. The line drawn in Fig. 2 indicates the system of the meantone tuning.

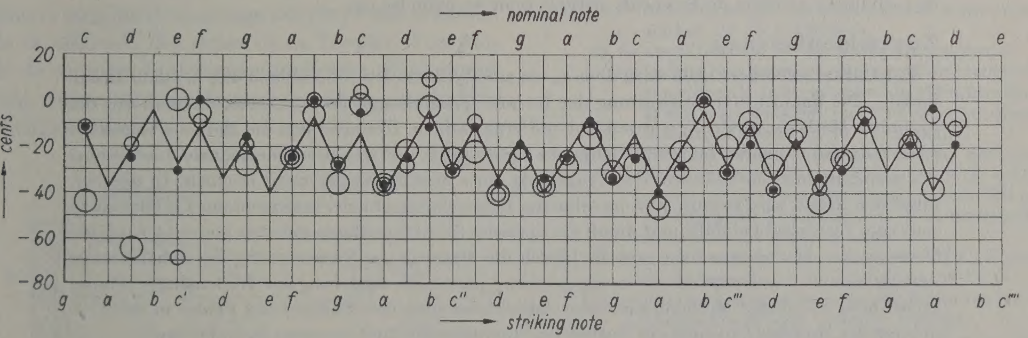

Fig. 2. Carillon Kampen

Table III

Carillon Kampen

Interval	gis- gis′	gis′- gis″	gis″- gis‴	average	meantone tuning base gis-14
prime	— 12	— 6	— 25	— 14	— 14
semitone		— 37	— 40	— 38	— 38
second	— 25	— 25	— 28	— 26	— 21
minor third		— 12	0	— 6	— 4
third	— 31	— 31	— 31	— 31	— 28
fourth	0	— 12	— 19	— 10	— 11
augm. fourth . . .		— 37	— 38	— 38	— 34
fifth	— 16	— 19	— 19	— 18	— 17
augm. fifth		— 34	— 34	— 34	— 41
sixth	— 25	— 25	— 31	— 27	— 24
dimin. seventh . .	0	— 9	— 9	— 6	— 7
seventh	— 28	— 34	— 31	— 31	— 31

4. The Middelstum carillon

Like Kampen and Delft, this carillon is also made in the meantone tuning. Calculations are given in Table IV. Searching for the average base, it was proved to be cis-3 cents. The greatest deviation is 9 cents and the average ± 4 cents. This justifies the conclusion that Hemony made these bells

Table IV

Carillon Middelstum

Interval	cis″- cis‴	cis‴- cis⁗	average	meantone tuning base cis-3
prime	0	— 6	— 3	— 3
semitone		— 22	— 22	— 27
second	— 3	— 6	— 5	— 10
minor third		+ 6	+ 6	+ 7
third	— 15	— 19	— 17	— 17
fourth	— 6	— 9	— 7	0
augm. fourth . . .	— 31	— 28	— 29	— 23
fifth	— 3	— 12	— 7	— 6
augm. fifth	— 31	— 25	— 28	— 30
sixth	— 12	— 9	— 11	— 13
dimin. seventh . .	0	+ 6	+ 3	+ 4
seventh	— 22	— 22	— 22	— 20

in the meantone tuning too. What does the above conclusion mean to our ears? From the early beginning, when the modern carillons were cast, they were made in equi-tempered tuning, which is now generally used. The popular opinion is that these carillons, even though excellent, have a different character and lack the charm of the HEMONY carillons. This is natural, as the tempered tuning enforced a levelling influence.

Could this be the key of the HEMONY secret? How about the practice? This has spoken for itself, for HEMONY carillons are still used very often and surely in more than one key. The meantone tuning permits many keys indeed; the carillon can be played in six keys in major as well as in minor, a range that is generally not surpassed, at least not in carillon music.

(Received 11th January, 1951.)

EMPLOI DES ONDES ULTRASONORES POUR L'ÉTUDE D'UN CHAMP AÉRODYNAMIQUE

Par Mlle M. MERLE*

Sommaire

Un faisceau d'ultrasons peut constituer un procédé de mesures instantanées et pratiques dans un champ aérodynamique. En effet, dans les mesures quantitatives obtenues par les méthodes optiques, le dépouillement des interférogrammes ou des striogrammes est long et compliqué. De plus ces méthodes ne permettent pas de séparer les gradients de densité rencontrés par un même rayon lumineux dans sa traversée de la veine fluide; l'étude détaillée à trois dimensions d'un champ aérodynamique autour d'une maquette est impossible. Nous montrons dans le présent article qu'un faisceau étroit d'ondes ultrasonores (dirigé normalement à la veine d'essai d'une soufflerie et au faisceau lumineux) visualisé par la méthode optique des stries, permet la mesure du nombre de Mach (par la détermination du déplacement du faisceau), permet encore de déterminer la variation de température du fluide (par la mesure de la variation de la longueur d'onde) et donne de plus d'utiles renseignements sur l'état du champ autour d'une maquette (degré de turbulence, nombre de Reynolds critique pour un cylindre, etc. . . .).

Zusammenfassung

Ein Ultraschallbündel kann dazu dienen, ein aerodynamisches Feld schnell und bequem auszumessen. Die quantitative Auswertung der Interferogramme und Striogramme, die man mit der optischen Methode erhält, ist zeitraubend und umständlich. Überdies sagt die Methode nichts aus über den Gradienten der Luftdichte längs des Lichtstrahls, und eine dreidimensionale Ausmessung des aerodynamischen Feldes in der Umgebung eines Modells ist gar nicht möglich. In der vorliegenden Arbeit wird gezeigt, daß ein schmaler Ultraschallstrahl, der senkrecht zur Luftströmung und zum Lichtstrahl einfällt und durch die optische Streifenmethode sichtbar gemacht wird, die Messung der Machschen Zahl erlaubt (durch die Messung der Verschiebung des Schallstrahls) und gleichfalls eine Temperaturmessung gestattet (durch die Änderung der Wellenlänge). Ferner erhält man mit dieser Methode nützliche Aufschlüsse über den Zustand des Feldes in der Umgebung des Modelles (Ausmaß der Turbulenz, Reynoldssché Zahl für einen Zylinder usw.).

Summary

A beam of ultrasonic waves may constitute a process of instantaneous and practical measurement in an aerodynamic field. In the quantitative measurement obtained by the optical methods, the verification of interferograms or striograms is indeed long and intricate. These methods, moreover, do not permit one to separate density gradients met by the same luminous ray in its crossing of the fluid. The detailed study in three dimensions of an aerodynamic field around a model is thereby impossible. We show in the present paper that a narrow bundle of ultrasonic waves (normally directed to the fluid stream of a windtunnel and the luminous beam, and made visible by the optical method of streaks) permits one to measure Mach's number (by determination of the displacement of the beam), permits one furthermore to determine the variation of the fluid temperature (by measuring the wave-length variation) and gives, besides, useful information about the state of the field around a model, of the degree of turbulence, Reynolds' criterion for a cylinder and so on . . .

---

* Travail effectué au CENTRE DE RECHERCHES SCIENTIFIQUES, INDUSTRIELLES ET MARITIMES — 66, rue St-Sébastien, Marseille.

1. Emploi des ondes ultrasonores pour l'étude d'un champ aérodynamique

L'étude par voie optique d'un champ aérodynamique présente un incontestable avantage sur les moyens mécaniques qui modifient l'écoulement étudié et ne peuvent donner instantanément une idée d'ensemble du phénomène. Toutefois, quelle que soit la méthode optique utilisée (des ombres, des stries, interférentielle), «l'image» obtenue dépend de l'épaisseur du canal traversé et ne permet pas de séparer les différents gradients de densité rencontrés le long du trajet lumineux. (Nous avons bien eu connaissance d'un système de striation avec focalisation fine, par MM. KANTROWITZ et TRIMPI [1], permettant de pouvoir obtenir une image formée uniquement par les gradients de densité dans un plan déterminé, mais le montage optique nécessite des lentilles anastigmatiques et achromatiques, et son utilisation est délicate et limitée.) De plus, les striogrammes, pas plus du reste que les interférogrammes, ne donnent facilement les répartitions des densités et par suite, pressions, températures, vitesses ou autres paramètres permettant l'étude du champ. Les méthodes de réduction des clichés sont longues, compliquées et d'une précision relative (surtout en ce qui concerne la méthode des stries). On voit donc l'avantage qu'il y aurait à doter une méthode optique de montage simple et très sensible, telle la méthode des stries ou de Toepler, d'un procédé de mesures également simple et suffisamment précis, permettant rapidement une étude qualitative et quantitative.

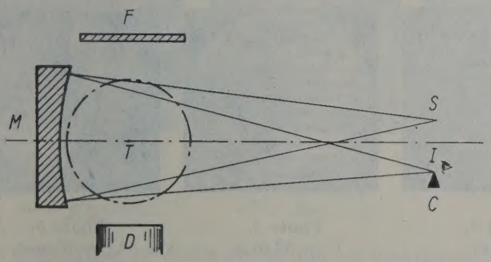

Fig. 1. Schéma du montage:
S = fente source de lumière placée un peu au dessus du centre de M,
M = miroir concave $\varnothing$ = 20 cm, $2f$ = 310 cm,
I = image de S dans laquelle se déplace le couteau C,
T = veine de la soufflerie $\varnothing$ 30 cm,
D = cylindre résonant, émetteur d'U.S.,
N = 23 000 c/s,
F = couche de feutre absorbant évitant la formation d'un spectre d'ondes stationnaires.

C'est dans ce but que nous avons utilisé un faisceau d'ultrasons envoyé normalement au faisceau lumineux et au champ aérodynamique que l'on veut étudier. La température peut être déduite de la fréquence connue des ultrasons et de la longueur d'onde mesurée; quant au nombre de Mach, il peut être obtenu, d'une manière approchée, par la mesure de la pente du bord du faisceau d'ultrasons [2]. De plus, l'aspect des ondes ultrasonores peut donner d'utiles renseignements sur l'état du champ aérodynamique autour d'une maquette, en des points et dans un plan bien déterminés.

2. Montage utilisé

L'émetteur d'ultrasons nous a été fourni par le Laboratoire d'Électroacoustique du C. R. S. I. M.; il est réproduit en Fig. 2.

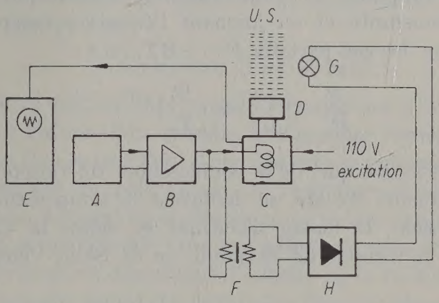

Fig. 2. Schéma de l'émetteur d'ultrasons:
A = hétérodyne pouvant fournir une tension sinusoïdale de 15 à 150 kc/s,
B = amplificateur de 90 watts alimentant C,
C = bobine fixe formant primaire d'un transformateur (dont la spire solidaire du cylindre vibrant D est le secondaire) sur le noyau d'un électroaimant alimenté en 110 V continu.
D = cylindre résonant, en duralumin. Ses vibrations commandent un microphone à condensateur dont il est l'électrode mobile. On peut contrôler sur l'oscillographe E la résonance et le maximum d'amplitude.
F = transformateur donnant 110 V H.F. à partir de la basse impédance alimentant C,
G = lampe au néon alimentée par F éclairée en synchronisme avec le cylindre vibrant,
H = redresseur dans le circuit de la lampe au néon, ne laissant passer qu'une seule alternance par période.

L'éclairage est modulé à la même fréquence que le faisceau sonore, ainsi une onde progressive paraît immobile et peut être observée ou photographiée avec tout le temps voulu.

3. Resultats obtenus

a. Mesure de la température

La température d'un fluide de vitesse notable ne peut être donnée par un thermomètre ordinaire; on peut utiliser des antennes thermométriques, mais elles doivent fonctionner dans des conditions aérodynamiques bien définies (forme, orientation) et leur présence perturbe le courant étudié. L'emploi d'un faisceau d'ultrasons ne présente pas cet inconvénient et peut permettre des mesures d'une grande précision.

La fréquence émise étant connue et constante, la longueur d'onde $\lambda = C/N$ varie quand varie la célérité du son dans le fluide; or cette dernière ne dépend que de la température absolue, d'où:

$$\frac{\lambda}{\lambda_e} = \frac{C}{C_e} = \left(\frac{T}{T_e}\right)^{1/2}$$

(λ_e, C_e, T_e = longueur d'onde, vitesse du son et température dans le hall extérieur au courant d'air.) En supposant la transformation adiabatique P/ρ^γ = constante et en joignant l'équation caractéristique des gaz parfaits $P = \rho R T$, on a:

$$\frac{P}{P_e} = \left(\frac{\rho}{\rho_e}\right)^\gamma = \left(\frac{T}{T_e}\right)^{\gamma/(\gamma-1)}$$

c'est-à-dire que, de la connaissance du rapport des longueurs d'onde, se déduisent la température, la pression, la masse spécifique et même la vitesse par la formule de Bernoulli ou de Saint-Venant.

a1. Vérification

Sur les photographies 1 et 2, un faisceau d'ultrasons, de fréquence 23 kc/s, est émis perpendiculairement à la veine d'essai de la soufflerie. Le courant d'air est dirigé de la droite vers la gauche. Les bandes claires correspondent aux maxima de pression de l'onde sonore, les bandes sombres aux minima. On peut déceler sur l'original une différence de 0,5 millimètre sur dix franges, c'est-à-dire une variation de l'ordre de $\lambda/150$ par longueur d'onde.

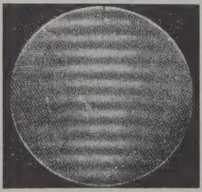
Photo 1.
$V = 0$.

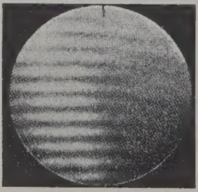
Photo 2.
$V = 83$ m/s.

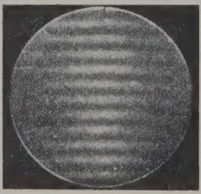
Photo 3.
$V = 0$.

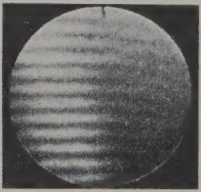
Photo 4.
$V = 83$ m/s.

Photo 5.
$V = 56$ m/s;
sans ultra-sons.

a2. Calcul

$$\frac{P}{P_e} = \left(\frac{T}{T_e}\right)^{\gamma/(\gamma-1)} \quad \text{ou} \quad \frac{T}{T_e} = \left(\frac{P}{P_e}\right)^{(\gamma-1)/\gamma}$$

Si l'on prend P_e = pression réservoir = 1,033 kg/cm².

T_e = température réservoir ≈ 288 °K,

$\Delta P = 0,043$ pour une vitesse de courant de 83 m/s,

$$\text{d'où } P = 1,033 - 0,043 = 0,990,$$

$$\gamma = 1,404$$

$$\frac{T}{T_e} = \left(\frac{0,990}{1,033}\right)^{\frac{0,404}{1,404}} = 0,988,$$

$$\text{et } \left(\frac{T}{T_e}\right)^{1/2} = \frac{\lambda}{\lambda_e} = 0,994.$$

C'est bien l'ordre de grandeur du résultat expérimental. Mais nous ne prétendons pas que, tel quel, le système employé soit suffisamment précis pour donner la température du fluide ou, ce qui revient au même, la célérité locale du son; car nos stries ne sont pas suffisamment rapprochées, des mesures précises demanderaient des fréquences d'ultrasons plus élevées et des vitesses de courant d'air plus grandes, afin que les gradients de température soient plus forts. Toutefois, ces clichés montrent que même avec de faibles nombres de Mach et des longueurs d'ondes ultrasonores nettement trop grandes, le phénomène est déjà décelable.

b. Mesure du nombre de Mach

On peut, à partir de la température, connaître la célérité du son dans l'air de la veine et par suite le nombre de Mach $M = V/C$, V étant donné par le pitot. Mais on peut essayer de le déterminer directement grâce à la remarque suivante: Quand la vitesse du courant d'air augmente, le faisceau se déplace vers l'aval du courant d'air (c'est-à-dire vers la gauche), comme le montrent les photographies 3 et 4.

La vitesse de déplacement horizontal des ondes est V = la vitesse du courant d'air, la vitesse verticale est C = la vitesse locale du son.

La frontière du faisceau sonore (d'ailleurs assez floue sur nos clichés) s'incline donc par rapport à la verticale d'un certain angle α tel que:

$\operatorname{tg} \alpha = V/C = M =$ nombre de Mach de l'écoulement.

On trouve que cet angle α, déterminé par le calcul (connaissant la température du hall et les pressions), est bien de l'ordre de grandeur de celui que l'on peut observer sur les photographies.

b1. Vérification

Photographie 4; $V = 83$ m/s, $P = 0{,}043$ kg/cm², α est de l'ordre de 13 à 14°.

b2. Calcul

$\frac{T}{T_e} = 0{,}988$ (ainsi que nous l'avons vu plus haut).

$T_e = 288^0$ K d'où $T = 288 \times 0{,}988 = 284{,}5$.

La célérité du son à cette température est égale à:

$$C = C_0 \sqrt{\frac{T}{T_0}} = 331 \sqrt{\frac{284{,}5}{273}} = 337{,}9 \text{ m/s},$$

$$M = \operatorname{tg} \alpha = \frac{83}{337{,}9} = 0{,}245, \qquad \alpha \approx 13^0\,45'.$$

La vérification est assez bonne, mais nous devons dire que, plus encore que pour la mesure des longueurs d'onde, l'angle α ne peut être mesuré avec précision sur les clichés ci-dessus (nous avons pris pour ligne de pente déterminant la frontière du faisceau d'ultrasons, une cassure, sorte de thalweg dans les stries). Cette difficulté vient de ce qu'il est impossible de fixer nettement les frontières du faisceau; la partie centrale est plus fortement visualisée que les parties marginales qui vont en s'estompant, car notre faisceau est circulaire et d'épaisseur optique non constante.

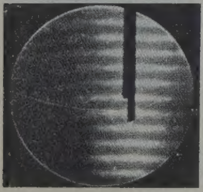

Photo 6.
$V = 0$;
avec ultra-sons.

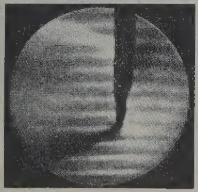

Photo 7.
$V = 27$ m/s;
avec ultra-sons.

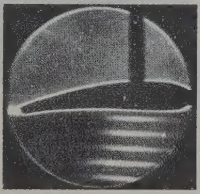

Photo 8.
$V = 0$.

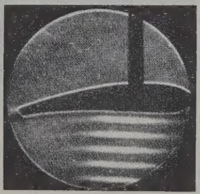

Photo 9.
$V = 19$ m/s.

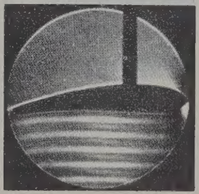

Photo 10.
$V = 59{,}5$ m/s.

c. Striogrammes de maquettes diverses

A noter que les supports des maquettes visibles et dirigés vers le haut, sont en dehors de la veine fluide et ne la perturbent pas. Les stries sombres ou claires du champ ne représentent pas les lignes de courant mais les variations de la pression.

c1. Plaque mince placée perpendiculairement au courant d'air (photos 5, 6 et 7).

On peut observer (photo 7) l'aspect tourmenté et élargi des stries claires à l'amont de l'obstacle, contrastant brusquement avec la finesse de celles qui sont en aval, dans le sillage de la plaque (zone de dépression constante).

c2. Profil d'aile Joukowsky 430 (photos 8, 9 et 10)

En comparant les photographies rangées suivant la vitesse croissante, on peut remarquer: le déplacement progressif du faisceau d'ultrasons vers la queue de l'aile, le faisceau d'ondes réfléchies par la maquette, et enfin la régularité des stries car le corps est bien profilé.

c3. Cylindre ∅ = 60 mm

Nous savons qu'il existe deux régimes d'écoulement autour d'un cylindre. Au premier régime, les filets fluides décollent à une distance angulaire d'environ 80° du pôle amont du cylindre; au second régime, le point de décollement est reculé en arrière, parfois jusqu'à 60°, et même moins, du pôle aval — cette position dépendant d'ailleurs de la turbulence du courant amont. De ce fait, le sillage est beaucoup moins large au voisinage du cylindre.

Quand on augmente progressivement la vitesse du courant d'air, le premier régime subsiste jusqu'à une valeur critique V_c de la vitesse; puis, plus ou

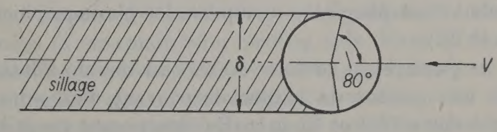

Fig. 3. Premier régime.

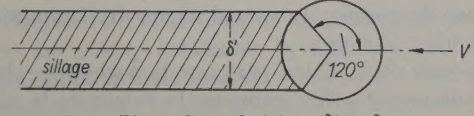

Fig. 4. Second régime ($\delta' < \delta$).

moins brusquement, la trainée subit une chute importante (C_x passe de 1,2 à 0,3 environ), le second régime d'écoulement s'établit. On définit un nombre de Reynolds critique qui sépare le premier du second régime et qui peut servir de critère de turbulence d'une soufflerie. Car Prandtl et Wieselsberger expliquent ce «retard» au décollement par le fait que la couche limite de laminaire est devenue turbulente avant le point de décollement. En effet, une perturbation quelconque de la couche limite suffit pour déclencher la chute brusque du C_x caractéristique du passage du premier au second régime. En conséquence, plus le courant d'air amont est turbulent, plus petit est le nombre de Reynolds critique (tout au moins tant que les phénomènes de compressibilité ne sont pas prépondérants). Mais outre la turbulence du courant d'air, la rugosité de la surface du cylindre agit sur la valeur du nombre de Reynolds critique, si bien que lorsqu'on se sert du cylindre ou de la sphère pour caractériser la turbulence d'une soufflerie, on doit utiliser une même maquette et le même appareillage.

La méthode ordinaire des stries nous a permis de déterminer «visuellement» la valeur approchée de ce nombre de Reynolds critique en fonction de la turbulence de la soufflerie ou de l'état de surface de la maquette. Nous avons également pu évaluer la durée du régime transitoire, qui sépare le premier du second régime et nous avons trouvé qu'il était d'autant plus étendu que la turbulence du courant amont était plus forte (comparer les photographies 11 et 12).

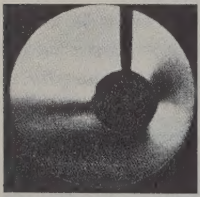
Photo 11.
$V = 75{,}4$ m/s;
premier régime.

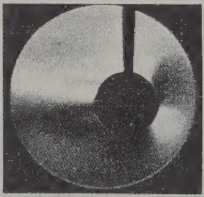
Photo 12.
$V = 81$ m/s;
second régime.

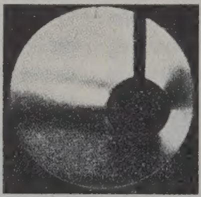
Photo 13.
$V = 83$ m/s;
régime transitoire.

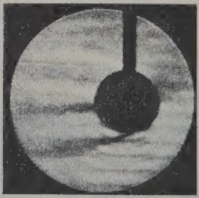
Photo 14.
Premier régime.

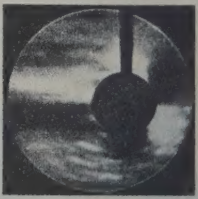
Photo 15.
Second régime.

Le passage du premier au second régime s'étale sur une gamme de vitesse de courant d'air comprise entre 75,4 et 81 m/s. En interposant un grillage dans le collecteur de la soufflerie et, toutes choses égales d'ailleurs, nous avons trouvé que le passage du premier au second régime était compris entre 67 et 77,5 m/s.

On voit donc, d'une part que la turbulence du courant amont a fait diminuer la valeur de la vitesse pour laquelle le régime transitoire commence à s'établir (67 au lieu des 75,4), d'autre part que la gamme des vitesses de celui-ci (81—75,4 = 5,6 et 77,5—67 = 10,5) est nettement plus étendue pour un courant plus turbulent.

En diminuant la rugosité de la maquette, nous avons pu maintenir le premier régime au-delà des valeurs de la vitesse trouvées ci-dessus. C'est ce que montre la photographie 13 où le second régime d'écoulement n'est pas encore établi bien que la vitesse du courant d'air soit déjà de 83 m/s.

Si on introduit maintenant un faisceau d'U.S. dans le champ on obtient les photos 14 et 15.

On remarquera:

a. au dessous de la maquette, les ondes réfléchies par celle-ci;

b. en haut et à gauche (photo 15), les ondes sonores qui ont traversé le sillage bien qu'elles n'apparaissent pas dans celui-ci du fait de la diffusion due à l'état tourbillonnaire de cette zone. Par contre elles sont légèrement visibles dans le premier régime d'écoulement (photo 14).

Ces photographies ne permettent pas encore de mesures précises ni l'emploi de maquettes à trois dimensions; toutefois, ces résultats sont encourageants car ils prouvent la sensibilité de la méthode. Afin d'obtenir de meilleurs résultats (notamment pour la mesure précise de la température), nous montons actuellement un émetteur d'ultrasons de fréquence nettement plus élevée, donnant des stries plus rapprochées et plus contrastées.

(Reçu le 8 Mars 1951.)

Bibliographie

[1] Kantrowitz, A. and Trimpi, R., A sharp focusing Schlieren system. J. Aero Sci. **17** [1950], 311—314.

[2] Marlow, D., Nisewanger, C. and Cady, W., A method for the instantaneous measurement of velocity and temperature in high speed air flow. J. appl. Phys. **20** [1949], 771—776.

[3] Guienne, P., Qualification de la turbulence en soufflerie par le nombre de Reynolds critique d'une sphère ou d'un cylindre. Groupement français pour le développement des recherches aéronautiques; (GRA Rapport technique No 3/1940).

THE SUBJECTIVE CALIBRATION OF BONE-CONDUCTION RECEIVERS FOR HEARING AIDS

by E. W. Ayers and J. Y. Morton
Post Office Research Station, Dollis Hill, London

Summary

To design a bone-conduction hearing aid it is necessary to know how loud a sound is produced by a given input to a receiver, but subjective calibrations by normal observers are unreliable as a guide to performance with deaf subjects. The influence of an intact air-conduction path on the subjective sensitivity of a bone-conduction receiver may be obviated by a method described, which simulates the effects of complete middle-ear deafness. Calibrations effected by this method using normal observers should be directly applicable to deaf subjects with serious middle-ear defects, but with substantially normal inner ears. Such subjects constitute the majority of those for whom bone-conduction aids are likely to be useful.

Sommaire

Pour faire un appareil facilitant l'écoute par conduction osseuse, il est nécessaire de connaître quelle est l'intensité physiologique du son émis pour une puissance donnée d'entrée au récepteur, mais on ne peut pas se fier à des étalonnages subjectifs faits par des observateurs normaux pour savoir ce qui se passe dans le cas des sujets sourds. L'influence de la transmission directe par l'air sur la sensibilité subjective d'un récepteur à conduction osseuse peut être évitée par la méthode décrite, qui simule les effets de la surdité complète de l'oreille moyenne. Les étalonnages effectués par cette méthode utilisée par des observateurs normaux seraient immédiatement applicables aux sujets sourds avec défauts sérieux de l'oreille moyenne, mais avec des oreilles internes absolument normales. De tels sujets constituent la majorité de ceux qui sont susceptibles d'utiliser les appareils à conduction osseuse.

Zusammenfassung

Um eine auf Knochenleitung beruhende Hörhilfe zu konstruieren, muß man wissen, welche Lautstärke erzeugt wird, wenn die Spannung am Empfänger vorgegeben ist. Subjektive Eichung durch normalhörende Personen gestattet jedoch keine zuverlässigen Schlüsse auf das Verhalten des Apparates bei Schwerhörigen. Durch die hier beschriebene Methode, bei der vollkommene Mittelohrtaubheit nachgeahmt wird, kann der Einfluß der Luftschallübertragung durch das gesunde Mittelohr auf die subjektive Empfindlichkeit eines Körperschallempfängers ausgeschaltet werden. Eichungen, die in dieser Weise von normalhörenden Personen ausgeführt werden, sollten sich direkt auf taube Personen mit schweren Mittelohrschäden, aber im wesentlichen gesundem Innenohr, übertragen lassen. Dies ist aber gerade die Mehrzahl der Patienten, denen Knochenleitungshörer helfen können.

1. Introduction

Most of the portable hearing aids now available use air-conduction receivers of either the "headphone" or insert type. A number of aids, however, use bone-conduction receivers which are worn behind the ear, in contact with the mastoid process, and stimulate the organ of hearing by mechanical vibrations transmitted through the skull. Bone-conduction aids appear to be useful where there is severe middle-ear deafness, especially if air-conduction receivers are medically undesirable, but up till now their design has remained largely empirical.

A considerable amount of research, in this country and elsewhere, has been devoted to the alleviation of deafness by sound amplification. The report M.R.C. No. 261 [1] of a committee of the Medical Research Council gives clear guidance in the design of air-conduction hearing aids. Many of the principles set down therein could be applied to bone-conduction aids if the subjective performance of receivers when used by the deaf could be reliably assessed.

2. Subjective calibrations

Subjective calibrations of air-conduction receivers are readily obtainable by adjusting the electrical input until an observer adjudges the resultant sensation equal to that produced by a known free sound field set up by a loudspeaker. The ratio of electrical input to equivalent free-field sound pressure is a function of frequency but independent of loudness level, since the non-linear relationship between loudness and intensity applies equally to the two sounds under comparison. The loudness corresponding to any free-field intensity may be found by reference to published data.

A similar method may be used for bone-conduction receivers, but the sensation experienced by the normal observers necessarily used is the resultant of a number of effects, including that of the appreciable air-borne sound field commonly associated with such receivers. Some of these effects are modified or absent in the deaf subjects who are the ultimate users, and neglect of this fact would invalidate the calibration.

3. Peculiarities of bone-conduction

Before attempting to devise a more realistic method of calibration, some well-known peculiarities of bone-conduction may with advantage be recorded:

a. The vibrating bone-conduction receiver and the side of the skull set up air-borne sound fields which may contribute to the total sensation through normal air-conduction channels.

b. With normal subjects the apparent bone-conduction sensitivity rises by up to 25 db at low frequencies if the ear canal is plugged [2]. This "occlusion effect," which is discussed further in section 5, does not appear if there is a large air-conduction loss.

c. At certain frequencies the apparent position of the sound produced by a bone-conduction receiver may shift from the ear adjacent to the receiver to the remote ear, perhaps as a result of changes in the vibration pattern of the skull.

d. Judgement of loudness equality between sounds from receiver and loudspeaker is hampered by pitch and tone quality differences, even though the excitations have identical frequencies and waveforms. Differences are greatest at low frequencies where the bone-conduction sensation changes in character.

e. Bone-conduction sensitivity changes with the pressure and position of the receiver on the head, and with the state of relaxation of neck and face muscles. The transmission characteristics of the bone structure, and especially of the mastoid process, which is full of air cells, vary widely from subject to subject.

Effects a. and b. depend on the proportion of hearing loss attributable to middle-ear defects. Effect c. normally appears only over narrow frequency bands in which bone transmission may be anomalous. For the present purpose readings affected by it have been disregarded, especially as many deaf subjects have effective hearing in one ear only. Effects d. and e. are common to normal and deaf subjects and should be covered by standardisation of test conditions and statistical treatment.

4. Assumed conditions

Sufficient is not known of the mechanism of bone-conduction hearing to establish a fundamental basis of calibration valid for all purposes. Consideration of practicable power output and of the relative sensitivity of air- and bone-conduction receivers suggests that the main application of bone-conduction hearing aids is to cases of severe middle-ear deafness where the inner ear is substantially normal, so in the following sections these conditions will be assumed. The design of hearing aids for this field may be based on calibrations by normal observers if the method described below is used to neutralise effects dependent on the air-conduction mechanism when listening to the bone-conduction receiver. Such calibrations are not necessarily appropriate for other purposes such as audiometry or clinical diagnosis of subjects with every variety and degree of hearing impairment.

5. Preliminary experiments

Preliminary experiments were made to assess the magnitudes of unwanted effects and devise means for eliminating them. Though the method evolved is not restricted to any one type of receiver, all measurements were made with small hearing-aid type receivers. These consist of an outer casing which is held against the mastoid process by a spring headband, and contains a heavy electro-mechanical drive unit. The case is vibrated by the inertia forces developed against the reaction of this mass.

5. 1. Air-borne radiation from receiver

When the receiver was lifted away from the head to suppress bone vibration the loudness of the sound did not fall to zero. At frequencies above 1500 c/s the change was quite small, suggesting that in the normal wearing position air-borne sound was comparable with bone-conducted sound. An alternative explanation that the change in mechanical loading allowed the receiver to radiate more strongly was shown to be insufficient by monitoring with a microphone.

Screening failed to stop the air-borne field reaching the observer's ear without impeding comparison with the free sound field, or introducing occlusion effects. Ignorance of the relative amplitudes and phases of wanted and unwanted stimuli at the inner ear prevented any attempt at calculating the effects. An auxiliary sound source was therefore used to cancel the sound pressure observed by a probe microphone at the entrance to the ear canal with the receiver lifted away from the head, and a complete subjective null was obtained at the same time. It was hoped therefore to balance out the air-borne radiation with the receiver in its normal position by reference to the probe microphone even though a subjective null would not then appear. Direct radiation to the remote ear fortunately appeared to be negligible, though this could have been allowed for by duplicating the equipment.

During the balancing experiments it was found that with the receiver touching the head some of the sound pressure seemed to come from a source within the ear canal. This was confirmed with the receiver held between the teeth so that direct radiation observed near the ear was negligible. The internal radiation was obviously due to the bone vibrations set up by the receiver, and possible sources seemed to be the bony walls of the canal itself, or the ear drum driven by inertia reaction from the ossicles.

5. 2. Occlusion effect

Either of the preceding assumptions was consistent with the occlusion effect. If the canal walls were vibrating a greater pressure would be set up with the entrance closed to form a high-impedance cavity than with it open. In a normal ear this pressure would act on the drum to increase the total sensation. The effect would be greatest at low frequencies and negligible at high frequencies where the impedance of even the closed canal would be small. Following the second assumption it might be supposed that part of the bone-conduction sensation in normal subjects was caused by inertia forces between ossicles and oval window. Occlusion of the ear canal would change the impedance presented to the ear drum and modify these forces.

5. 3. Neutralisation of pressure at ear drum

With severe middle-ear deafness the bone-conduction signal would be unaffected by sound pressures at the ear drum or changes in impedance of the external ear cavity. Equivalent conditions for normal observers could be obtained by ensuring that there was no sound pressure on the ear drum when using the bone-conduction receiver. This object was achieved with the balancing technique described above by extending the microphone probe with soft rubber tubing almost to the drum. A check with the end plugged showed negligible stray pick-up due to this tube lying on the vibrating walls of the canal. Up to 3000 c/s no difference was detectable in the loudness of the bone-conduction signal when the auxiliary balance was made with the probe first at the drum and then at the opening of the canal, so the latter position was chosen for subsequent tests to reduce risk and strain for the subject. The balancing technique was applied only to the ear adjacent to the bone conductor, since it was intended to utilise only observations which were substantially unaffected by stimulation reaching the remote ear.

5. 4. Other effects

The shift in apparent position of the sound source was experienced by many observers, usually only over narrow frequency bands. Measurements on two subjects who shewed the effect over a wide frequency range were excluded in calculating the means. However, further study of this effect is desirable. Harmonic levels in the free-field sound pressure and in the receiver input signals were always at least 40 db below fundamental, but all subjects noticed tone quality and pitch differences except for frequencies near 2000 c/s. The effect was greatest at low frequencies and high amplitudes and may have been partly due to harmonics generated in the receiver, but similar differences have been noticed with air-conduction receivers known to produce very little distortion. At low frequencies, especially near mechanical resonance of the receiver, subjects reported that the vibration of the head could be felt, apart from the sound sensation caused, and a feeling of nausea resulted from prolonged exposure.

6. Calibration procedure

The methods evolved from the preliminary experiments were used in a full-scale test to obtain subjective calibrations for sample receivers. Sixteen male subjects were used with eight receivers of one type, each tested twice. A description of the experimental equipment and test procedure, and typical results obtained, are given below.

6. 1. Equipment

Observers were comfortably seated in a chair facing a 20 cm diameter loudspeaker in one wall of a non-reverberant room. A rest kept the head in the correct position in the sound field, with the ears 1.20 m from the loudspeaker, while allowing the neck muscles to be relaxed. Observers were instructed to keep the mouth closed, with the teeth touching but not clenched. The receiver was placed on the head with a large sponge rubber pad under the free end of the headband to prevent vibrations transmitted along the latter from reaching the remote ear. The force with which the receiver was held against the head was set to 440 ± 20 grams weight, and the position adjusted by the subject for loudest reception with a speech input from a gramophone record, taking care that no part of the pinna touched the receiver or headband. This allowed a more reliable judgement of the best position for all speech frequencies than the use of a single tone.

A two-position switch on the left arm of the chair switched the test tone to either receiver or loudspeaker, and the input level in the latter position could be varied continuously over a range of 20 db by a control fixed to the right arm of the chair. Adjacent to this control was a three-position switch to vary the level by ± 2 db as an aid to judgement. Instructions and comments were passed over a two-way intercommunication system between the non-reverberant room and adjacent control room.

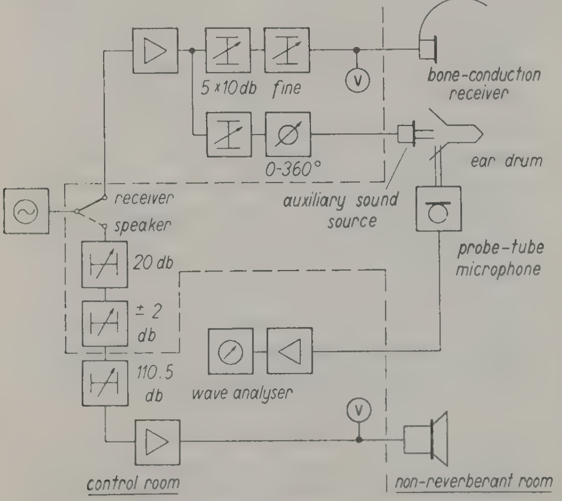

Fig. 1. Arrangement of apparatus for experiment.

The equipment to the left of the broken line in Fig. 1 was housed in the control room. The oscillator was switched electronically to either receiver or loudspeaker, through time-delay circuits to avoid clicks. The switching was normally effected by the observer, although the operator in charge had an over-riding control. Attenuators were provided to adjust the inputs to the loudspeaker and receiver, and the actual voltage across the loudspeaker terminals, which depended also on the setting of the observer's control, could be read on a voltmeter. The auxiliary sound source, consisting of a small receiver coupled to a tube directed into the ear of the observer, was fed from the receiver circuit through an adjustable attenuator and phaseshifter, both with fine controls. The presence of these auxiliary circuits made it convenient to vary the input to the loudspeaker, rather than the receiver, when making a comparison.

Acoustic and magnetic pick-up by the probe microphone from the bone-conduction receiver resulted at first in a false null when balancing out the sound pressure at the ear drum. On replacing the normal capillary probe by a 0.6 m length of 3 mm bore brass tube, which had a lower attenuation and removed the microphone and its cable from the immediate vicinity of the receiver, a signal-to-pick-up ratio of better than 30 db was achieved. Interference from general background noise was reduced by observing the microphone output on a narrow-band wave analyser.

6. 2. Test procedure

To avoid fatigue, tests on each subject were spread over four sessions each lasting not more than 20 minutes, with rests of at least half an hour between. The first session was used to test air-conduction hearing in both ears, for frequencies between 200 and 4000 c/s, with a Western Electric Audiometer Type 6 BP. Selected subjects came within the range 5 db hearing loss to 15 db gain relative to the zero on this instrument.

In the second session the subject was introduced to the controls and given some practice in making loudness balances. The input to the receiver was then raised in 10 db steps, keeping the frequency constant at 1000 c/s, and the increments of equivalent free-field pressure used to check the subject's powers of judgement. The receiver pressure and position were then adjusted, and for all remaining tests a constant voltage was maintained across the terminals. Attenuation was introduced at random into the loudspeaker circuit to force the observer to make a substantial readjustment of his level control for each judgement. Balances were obtained at frequencies of 1000, 750, 500, 300, and 200 c/s, where the auxiliary sound source was not used as it was found not to influence the results.

For the third and fourth sessions the receiver pressure and position were readjusted. An input was applied and the controlling operator set the auxiliary sound source to reduce the output from the probe microphone at least 20 db before the subject was asked to make his balance. The probe microphone output was checked after each balance to make sure that the subject had not moved meanwhile. Measurements were made at 1000, 1250, 1500, 1760, and 2000 c/s during the third session, and at 2500, 3000, 3500, and 4000 c/s during the fourth session. Doubtful readings were checked before a session finished.

The loudspeaker was calibrated by a standard condenser microphone so that voltage readings could be converted into unobstructed free-field sound pressures at the position of the subject's head. Actual pressures at the subject's ears were of course somewhat greater at the higher frequencies due to diffraction.

6. 3. Results and accuracy

Results from the right ears of 16 male subjects, with a mean hearing acuity 5 db above normal are shewn in Figs. 2 and 3. Fig. 2 shows a mean frequency-response curve in terms of equivalent free-field sound pressure for a constant input voltage, for eight receivers of one type, each tested twice. Fig. 3 is a typical calibration by one subject. The linear relationship between equivalent free-field sound pressure and input voltage is illustrated by Fig. 4, from which the mean differences between subjects have been eliminated.

Calibration checks of the comparison sound field at the end of each day's work revealed a mean error of ± 0.2 db, and a maximum of 0.5 db over the whole frequency range. The linearity measurements shewn in Fig. 4 were based on the means of up to five readings for each subject and input level. From the variation of these readings among themselves the standard deviation from the mean reading for immediate repeat balances, and for day-to-day repeats, have been calculated, and are shewn in the Table below.

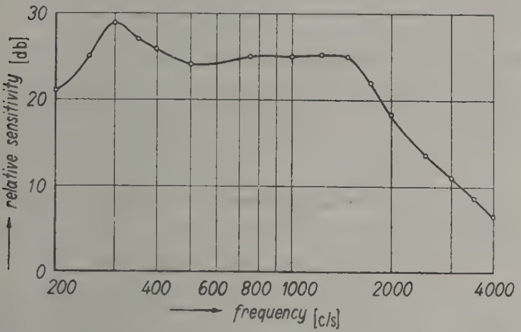

Fig. 2. Mean sensitivity v. frequency of 8 receivers on 16 subjects.

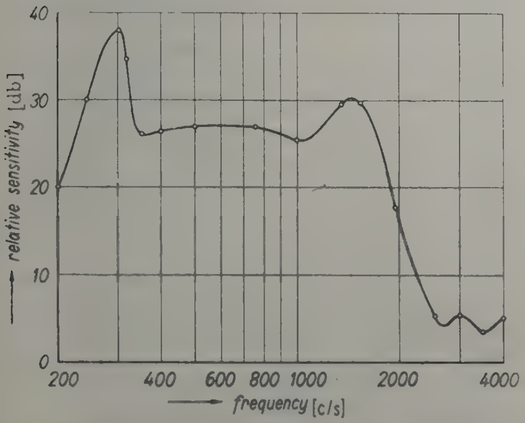

Fig. 3. Typical calibration by one subject on one receiver.

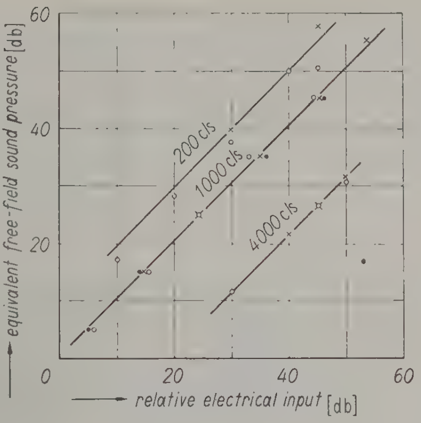

Fig. 4. Linearity.

Standard deviation from mean of subjective sensitivity measurements in db

Frequency [c/s]	Immediate repeats	Day-to-day repeats
200	1.6	5.9
500	0.4	3.4
750	0.9	2.8
1000	0.6	3.9
2000	1.0	—
4000	1.3	—

The greater variation with day-to-day repeats is attributed to alterations in position of subject and receiver, changes in hearing acuity, and shifting mental standards in assessing the balance point. The last effect was particularly troublesome at low frequencies where the receiver and loudspeaker tones differed greatly in subjective quality.

Acknowledgements

Acknowledgement is made to the Engineer-in-Chief of the General Post Office and to the Controller of H. M. Stationery Office for permission to publish this paper, and to the authors' colleagues who assisted with the experimental work.

(Received 26th December, 1950.)

References

[1] Medical Research Council: Special Report Series No. 261. "Hearing Aids and Audiometers." Report of the Committee on Electro-Acoustics. H. M. Stationery Office, London, 1947.
[2] WATSON and GALES, J. acoust. Soc. Am. **14** [1943], 207.

SOUND ABSORPTION BY SLIT RESONATORS

by J. M. A. Smits and C. W. Kosten

Laboratorium voor Technische Physica der Technische Hogeschool, Delft, Holland.

Summary

A theory is presented that permits the approximate calculation of the frequency of maximum sound absorption of constructions consisting of a perforated rigid panel mounted at a short distance before a rigid wall, the perforation being a system of infinitely long parallel and identical slits. The precision seems to meet all practical requirements. The results of some experiments, corroborating the theory, are given. A comparison is made between slit perforation and perforation with circular holes. For both cases design charts are given.

Sommaire

On propose une théorie permettant de calculer d'une manière approximative la fréquence du maximum d'absorption des structures constituées par un panneau rigide perforé, placé à petite distance devant une paroi rigide, la perforation étant un système de longues fentes parallèles et identiques. La précision atteinte semble suffisante pour tous les besoins de la pratique. On donne les résultats de quelques essais qui valident la théorie. On compare la perforation à fentes et celle à orifices circulaires. Des graphiques d'utilisation sont donnés pour ce dernier cas.

Zusammenfassung

Es wird eine Theorie dargelegt, die es erlaubt, die Frequenz der maximalen Schallabsorption eines Schlitzabsorbers näherungsweise zu berechnen. Es handelt sich bei diesen Absorbern um harte, mit unendlich langen, parallelen, gleichartigen Schlitzen versehene Platten, die in kurzem Abstand von einer starren Wand angebracht sind. Die Genauigkeit scheint allen praktischen Anforderungen zu genügen. Die Ergebnisse einiger Messungen werden mitgeteilt; sie bestätigen die Theorie. Es werden Perforationen mit Schlitzen und mit Löchern miteinander verglichen. Für beide Fälle werden Konstruktionsdiagramme angegeben.

1. Introduction

Sound absorbing materials consisting of a perforated rigid panel at some distance before a rigid wall, the air gap being filled with a suitable porous material, are in wide-spread use.

Mathematically they can often be treated as a simple acoustic resonator [1]: the mass, the resistance and the rigidity of the resonator govern the behaviour. The rigidity is simply inversely proportional to the volume of the resonator (distance panel-wall), the resistance can be varied by choosing adequately the filling material. The mass depends upon the perforation. In the case of circular holes the problem is solved with high accuracy [2], [3]. Sometimes a perforation in the form of parallel identical slits is used [4]. A simple theory describing their behaviour is lacking, however. This hampers the development of such constructions. In this article this problem is dealt with.

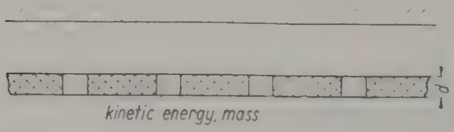

Fig. 1. Perforated panel construction.

2. Literature, line of approach

Consider the well known case of a panel of thickness d, perforated with a system of circular holes in some regular way, backed at some distance by a rigid wall (see Fig. 1). If this system is set into vibration by a sound wave impinging normally to it, the kinetic energy of the system is mainly to be found in the holes and their close neighbourhood. Owing to the spread of the flow of air inside the air gap the kinetic energy in the gap is negligible, i. e., whether the air inside the gap has a density that differs from zero or not does not materially influence the behaviour of the system. We may therefore concentrate our attention on the mass of air vibrating within the holes. The mass per hole is obviously $\rho S d$, where ρ is the density of air, S the surface of the cross section of the hole and d the thickness of the panel. For a panel of an infinitely small thickness the mass, according to this formula, would be zero. This turns out to be incorrect, which is reasonable on second thoughts, if one bears in mind that even in this case the kinetic energy is greater than without the panel at all. In order to allow for this kinetic energy a hypothetical mass $\rho S l$ is introduced; $l/2$ is called the end correction at either side. It will be clear from this that the same effect will be present in the case of finite thickness d of the panel. The mass in this case can be expected to be in excess of the previously mentioned value $\rho S d$ by an amount of the order of magnitude $\rho S l$.

For one circular hole in an infinite screen of finite thickness this problem has already been treated at length by Rayleigh, who gives a lower and upper limit for the end correction. Assuming the pressure to be constant over the cross section of the channel at either end he finds for the end correction at one side [2]

$$l/2 = {}^1/_4\, \pi R,$$

R being the radius of the hole, and he proves that the correct value can only be greater. The upper limit is determined on the assumption that the velocity is constant over the end cross section and turns out to be

$$\frac{l}{2} = \frac{8}{3\pi} R,$$

the difference between both solutions being 8%.

Ingård [5] and Nielsen [3] treated the case of a circular hole in a disk fitting in a circular tube, a case much nearer prevailing conditions in practical constructions (perforated panels) than the case of one single hole in an infinite plane. Ingård solved it assuming a constant velocity over the cross section. Nielsen takes for the velocity function over the cross section a linear combination of the constant velocity and the velocity distribution belonging to a constant pressure over the cross section; out of all possible linear combinations that one is chosen that makes the total kinetic energy a minimum.

The behaviour of one single slit of infinite length in a wall of infinite dimensions cannot be treated in the hydrodynamical way of Rayleigh. The reason has already been given by Pedersen [4] and is to be found in the fact that the slit problem is two dimensional (slow divergence of air flow), whereas the first problem (circular hole) is three dimensional (rapid divergence of air flow, small dimensions of the domain of appreciable kinetic energy).

The lower limit of the total end correction (assuming the pressure constant over the cross section) is found to be [6]

$$l = 0.515\, b + \frac{2}{\pi} \ln \frac{\lambda}{\pi b},$$

where b is the breadth of the slit and λ the wave length of the incident sound.

As far as is known to the authors the upper limit (assuming the velocity constant) has not yet been given in the literature. We should like to give here the result for this case without giving the rather lengthy derivation:

$$l = 0.588\, b + \frac{2}{\pi} \ln \frac{\lambda}{\pi b}.$$

The fact that the wavelength λ enters into the end correction means that the domain of appreciable kinetic energy is certainly not negligible in comparison with the wavelength. This implies that if a periodic system of infinite parallel slits in a wall is considered, in which the mutual distance of the slits is small in comparison with the wavelength λ the end correction will probably be a function of the mutual distance of the slits B.

In practice this is the problem to be solved; again an upper and a lower limit are desirable, if the true value is difficult to obtain. This is actually the case. In the next sections the problem will be solved using two hypothetical distributions of the velocity over the slit. The first is a constant velocity all over the slit which seems to give a suitable upper limit for the end correction. For the other distribution we have taken the one found by Lamb [7] for the hydrodynamical case of a fluid flowing through a periodic system of parallel slits in a thin screen. It is as yet uncertain whether this assumption does yield a lower limit, although there is some evidence to this effect (see sect. 7 and Table II).

We will distinguish between the two cases by referring to them as "constant velocity" and "constant pressure".

3. Behaviour of the air in the gap

If a plane sound wave, sound pressure p_i, impinges normally upon the panel, the pressure just in front of the panel would be $2p_i$ if the slits were absent. This is the acoustical "e. m. f." in our problem; it works upon two impedances, the impedance of the resonator (which one finds just before the panel looking towards the panel) plus the radiation impedance (found in the same position but looking backwards, the "e. m. f." being absent). These impedances have to be evaluated separately (this section and sect. 4.). For the moment the thickness d of the panel will be taken as zero, the influence of d not being zero is introduced very simply by the addition of an inertia term (see sect. 5.).

For the meaning of the symbols x, y, B, b and D we refer to Fig. 2. It can easily be shown by the procedure of parting of variables that the solution of circular frequency ω of the wave equation

$$\frac{\partial^2 p}{\partial x^2}+\frac{\partial^2 p}{\partial y^2}=\frac{1}{c^2}\frac{\partial^2 p}{\partial t^2} \qquad (1)$$

in our case is an expression, periodical in y, of the form

$$p=\sum_{n=0}^{\infty}\left[A_n \exp(\mathrm{j}k_n x)+B_n \exp(-\mathrm{j}k_n x)\right]\cdot$$
$$\cdot \cos b_n y \, \exp \mathrm{j}\omega t. \qquad (2)$$

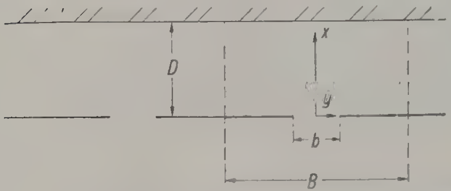

Fig. 2. To the derivation of the expression for the pressure inside the gap.

The factor $\exp \mathrm{j}\,\omega t$ can be included in A_n and B_n and therefore dropped. Terms in $\sin b_n y$ do not enter for reasons of symmetry. There is a relation between k_n, b_n and the circular wavenumber $k=2\pi/\lambda=\omega/c$, as appears from the substitution of equation (2) in (1) viz.

$$k_n^2+b_n^2=k^2. \qquad (3)$$

Moreover b_n is easily found from the periodicity, imposed by the problem,

$$b_n B=2\pi n, \text{ with } n=0,1,2\ldots \qquad (4)$$

and therefore by (3)

$$k_n=\pm \mathrm{j}k\sqrt{\left(\frac{n\lambda}{B}\right)^2-1}. \qquad (5)$$

The plus sign may be disregarded, it would imply an interchange of A_n and B_n. The unknown constants A_n and B_n in p must be determined by first deriving from (2) an expression for the particle velocity v and then taking into account the boundary conditions for the particle velocity v, imposed by the problem, namely,

a) at $x=D$, $v_x=0$;
b) at $x=0$, $v_x=0$ except in the slits where
(constant velocity) $v_x=u=\text{constant}$
(constant pressure) $v_x=u\dfrac{b}{B}\dfrac{\cos \pi y/B}{\left(\sin^2\frac{\pi}{2}\frac{b}{B}-\sin^2\pi\frac{y}{B}\right)^{1/2}}$

As mentioned above the latter expression is taken from Lamb [7]. The particle velocities resulting from the pressure p are easily found from the relation

$$-\operatorname{grad} p=\rho\frac{\partial \bar{v}}{\partial t} \text{ or } v_x=-\frac{1}{\mathrm{j}\omega\rho}\cdot\frac{\partial p}{\partial x} \qquad (6)$$

Condition a) yields then

$$A_n \exp(\mathrm{j}k_n D)=B_n \exp(-\mathrm{j}k_n D). \qquad (7)$$

Condition b) can be used by expanding the prescribed velocity distribution in a Fourier series

$$v_x=u\sum_0^{\infty}a_n \cos 2\pi n y/B=u\sum_0^{\infty}a_n \cos b_n y \qquad (8)$$

with the Fourier coefficients

(const. velocity) $a_0=\dfrac{b}{B}$ and $a_n=\dfrac{2}{n\pi}\sin n\pi\dfrac{b}{B}$

(const. pressure) $a_0=\dfrac{b}{B}$ and (9)

$$a_n=\frac{2b}{B}\,\mathrm{F}\left(n,-n,1,\sin^2\frac{\pi}{2}\frac{b}{B}\right)$$

where F is the common expression for a hypergeometric function; the latter coefficients can be derived from expressions given by Lamb [7]. Equation (8) must be identical with the Fourier series giving v_x for $x=0$ as computed from the pressure expression (2) with the aid of (6). This relates A_n and B_n of p to the known coefficients a_n of v_x and we finally find

$$p=-\mathrm{j}\rho c u\sum_0^{\infty}\frac{k a_n}{k_n}\frac{\cos k_n(x-D)}{\sin k_n D}\cos b_n y, \qquad (10)$$

and for $x=0$

$$p=-\mathrm{j}\rho c u\sum_0^{\infty}\frac{k a_n}{k_n}\cot k_n D \cos b_n y. \qquad (11)$$

We shall now do the same at the outside of the construction, which reduces to a study of the free radiation in a half infinite space of air, since the incoming wave is as yet disregarded.

4. The behaviour of the air outside, radiation

The radiation problem is much the same as that of section 3. The boundary condition $v_x=0$ for $x=D$ must be dropped however and is replaced by the condition that only outgoing waves are present ($A_n=0$). Thus

$$p=\sum_0^{\infty}B_n \exp(-\mathrm{j}k_n x)\cos b_n y$$

in which, again, b_n is governed by (4), k_n by (5).

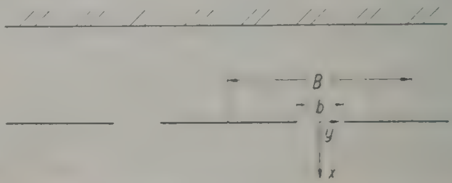

Fig. 3. To the derivation of the expression for the pressure outside the gap.

Along exactly the same lines as in section 3 we now compute for $x=0$

$$p=\rho c u \sum_{0}^{\infty} \frac{k a_n}{k_n} \cos b_n y. \tag{12}$$

5. The ratio of the incident pressure and the air velocity in the slits

The acoustical "e. m. f." $2p_i$ acts upon the impedances at the inside and at the ouside of the slits. If we draw up the equation of motion for a small volume of air $d \cdot dy \cdot 1$ in a slit (see Fig. 4) we obtain

$$(2 p_i + p_{out} - p_{in}) \mathrm{d}y = \mathrm{j}\, \omega \rho d \cdot \mathrm{d}y \cdot v_x. \tag{13}$$

p_{in} is given by (11), p_{out} by (12), v_x by (8) and (9).

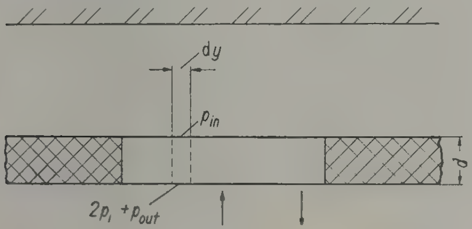

Fig. 4. To the equation of motion of the air in a slit.

All three quantities p_{out}, p_{in} and v_x are proportional to u. The ratio between the given incident pressure p_i and the resulting velocity u can, therefore, be computed from (13). This ratio should of course be independent of the ordinate y of the chosen air volume, but due to the approximate distribution of the velocity, assumed earlier, this will not be the case exactly. We can, however, require that (13) applies on the average, integrating it over the slit. Doing this, substituting at the same time (11) and (12), and finally replacing u by $-u$ in eq. (12) with a view to the direction of the x-axis chosen, we obtain

$$2 p_i b = \rho c u \int_{-b/2}^{+b/2} \left(\sum_{0}^{\infty} \frac{k a_n}{k_n} \cos b_n y - \right. \tag{13}$$

$$\left. -\mathrm{j} \sum_{0}^{\infty} \frac{k a_n}{k_n} \cot k_n D \cdot \cos b_n y \right) \mathrm{d}y + \mathrm{j}\omega\rho b d u.$$

For the first series we must take the minus sign for k_n in (5). The second series does not depend upon the sign of (5) chosen, so we take the minus sign of (5) for both series. After integration the whole expression may be rewritten:

$$2 p_i = \tag{14}$$

$$\left[\frac{\rho c k B}{\pi b} \sum_{0}^{\infty} \frac{a_n}{k_n} \frac{1}{n} \sin n\pi \frac{b}{B} (1 - \mathrm{j} \cot k_n D) + \mathrm{j}\omega\rho d \right] u.$$

It is advantageous to introduce another velocity instead of u, viz v, the mean velocity all over the panel, given by:

$$v = \frac{b}{B} u.$$

Furthermore we know

$k_0 = k = \omega/c \quad k_n = -\mathrm{j}\, k \sqrt{(n\lambda/B)^2 - 1} \qquad$ for $n > 0$

$b_0 = 0 \qquad b_n = 2 n\pi/B$

(constant velocity)

$a_0 = b/B \qquad a_n = \frac{2}{n\pi} \sin n\pi \frac{b}{B} \qquad$ for $n > 0$

(constant pressure)

$a_0 = b/B \qquad a_n = 2 \frac{b}{B} \mathrm{F}\left(n, -n, 1, \sin^2 \frac{\pi}{2} \frac{b}{B}\right)$ for $n > 0$

If we define a new real quantity R_n according to

$$k_n = -\mathrm{j}\, k R_n \; (n > 0) \text{ with } R_n = \sqrt{(n\lambda/B)^2 - 1}$$

and insert all this we obtain

(constant velocity)

$$2 p_i = v \left[\mathrm{j}\omega\rho \frac{Bd}{b} + \rho c - \mathrm{j}\rho c \cot k D + 2 \mathrm{j}\rho c \frac{1}{\pi^2} \left(\frac{B}{b} \right)^2 \cdot \right.$$

$$\left. \cdot \sum_{1}^{\infty} \frac{1}{R_n n^2} \sin^2 n\pi \frac{b}{B} (1 + \coth k D R_n) \right] \tag{15}$$

(constant pressure)

$$2 p_i = v \left[\mathrm{j}\omega\rho \frac{Bd}{b} + \rho c - \mathrm{j}\rho c \cot kD + 2 \mathrm{j}\rho c \frac{1}{\pi} \frac{B}{b} \cdot \right.$$

$$\left. \cdot \sum_{1}^{\infty} \frac{\mathrm{F}}{R_n n} \sin n\pi \frac{b}{B} (1 + \coth k D R_n) \right].$$

6. The equivalent impedance of the panel

If the panel had been a homogeneous plane with specific acoustic impedance z, we should have written as usual

$$2 p_i = (z + \rho c)\, v,$$

since then the radiation impedance would simply have been ρc. The equivalent specific acoustic impedance of the slit system is, therefore, found to be (compare (15))

(const. velocity)

$$z_{eq} = \mathrm{j}\omega\rho \frac{B}{b} d - \mathrm{j}\rho c \cot kD + 2 \mathrm{j}\rho c \frac{1}{\pi^2} \left(\frac{B}{b} \right)^2 \cdot$$

$$\cdot \sum_{1}^{\infty} \frac{1}{R_n n^2} \sin^2 n\pi \frac{b}{B} (1 + \coth k D R_n) \tag{16}$$

(const. pressure)

$$z_{eq} = \mathrm{j}\omega\rho \frac{B}{b} d - \mathrm{j}\rho c \cot kD + 2 \mathrm{j}\rho c \frac{1}{\pi} \left(\frac{B}{b} \right) \cdot$$

$$\cdot \sum_{1}^{\infty} \frac{\mathrm{F}}{R_n n} \sin n\pi \frac{b}{B} (1 + \coth k D R_n).$$

7. Discussion of the results, approximations

Equation (16) looks complicated but its physical interpretation is quite simple. To begin with the impedance is entirely imaginary, as it should be. The first term is a simple inertia term due to the mass of air in the slit, it needs no further explanation. The second term is a stiffness term, the well-known plane wave impedance of a layer of air backed by a rigid wall. If the air gap is very small in comparison with the wavelength λ (i. e. $kD \ll 1$) we can write

$$-\mathrm{j}\rho c \cot kD = -\frac{\mathrm{j}\rho c}{kD} = \frac{\varkappa p_0}{\mathrm{j}\omega D}, \tag{17}$$

which is the well-known expression for the impedance of an air spring of unit surface and thickness D. This approximation leads to errors in the resonance frequency smaller than 5% (10% in stiffness), if D is smaller than $0.1\,\lambda$, e. g. for frequencies up to 700 Hz, $D < 5$ cm; in most cases, therefore, this approximation is permissible. The third term is the most complicated one. It has inertia character and is built up of an inertia part originating inside the resonator (coth-part) and a part from the outer end correction (the 1-part). It is a function of b/λ, B/λ and D/λ. One of these variables can be cancelled by a rather good approximation. For $B < 0.5\,\lambda$, $R_n = \sqrt{(n\,\lambda/B)^2 - 1}$ can be simplified to $R_n = n\,\lambda/B$ for 5% error in resonance frequencies of practical constructions in unfavourable conditions. The terms in question reduce considerably:

(const. velocity)

$$\mathrm{j}\omega\rho \frac{1}{\pi^3}\left(\frac{B}{b}\right)^2 B \sum_1^\infty \frac{1}{n^3} \sin^2 n\pi \frac{b}{B}\left(1 + \coth 2\pi n \frac{D}{B}\right)$$

(const. pressure)

$$\mathrm{j}\omega\rho \frac{1}{\pi^2}\frac{B}{b} B \sum_1^\infty \frac{\mathrm{F}}{n^2} \sin n\pi \frac{b}{B}\left(1 + \coth 2\pi n \frac{D}{B}\right).$$

A further simplification were possible for $2\pi D/B > 2$, it being allowed, then, to put the coth equal to unity. Although this condition is in most cases fulfilled there is not much reason for this simplification since the remaining series, even then, must be tabulated or represented in a graph for practical use and it is a small complication to include the variable D/B as well. Resuming, we can write, only applying the harmless restriction $B < 0.5\,\lambda$,

$$z_{eq} = -\mathrm{j}\rho c \cot kD + \mathrm{j}\omega\rho B\left(\frac{d}{b} + \frac{l}{b}\right) \tag{18}$$

with

(const. velocity)

$$\frac{l}{b} = \frac{1}{\pi^3}\left(\frac{B}{b}\right)^2 \sum_1^\infty \frac{1}{n^3} \sin^2 n\pi \frac{b}{B} \cdot \left(1 + \coth 2\pi n \frac{D}{B}\right)$$

(const. pressure)

$$\frac{l}{b} = \frac{1}{\pi^2}\frac{B}{b} \sum_1^\infty \frac{1}{n^2} \mathrm{F}\left(n, -n, 1, \sin^2 \frac{\pi}{2}\frac{b}{B}\right) \cdot \sin n\pi \frac{b}{B}\left(1 + \coth 2\pi n \frac{D}{B}\right). \tag{19}$$

The quantity l/b is shown in Fig. 5 as a function of its variables b/B and B/D for the case of constant velocity; one curve for the case of constant pressure, viz. for $B/D = 0$, has been added suggesting that, at least for small values of B/D, there is not much numerical difference between both cases (see also Table II). For the convenience of the reader the results are also given in Table I.

If D is supposed to increase to infinity the coth tends to unity. The expression for the total end correction in the "constant pressure" case then simplifies to

$$l = \frac{2}{\pi^2} B \sum_1^\infty \frac{\mathrm{F}}{n^2} \sin n\pi \frac{b}{B},$$

for which a much simpler expression can be derived with the aid of formulae given by LAMB [7], viz.

$$l = \frac{2}{\pi} b \ln \operatorname{cosec} \frac{\pi}{2}\frac{b}{B}. \tag{20}$$

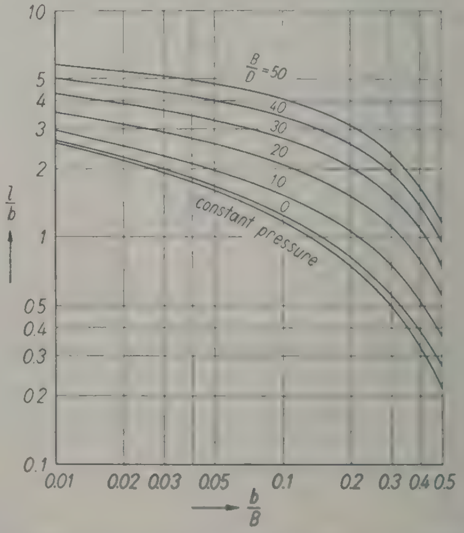

Fig. 5. The relative end correction of slits l/b as a function of b/B and B/D for "constant velocity" and as a function of b/B and $B/D = 0$ for "constant pressure".

Table I

The quantity l/b as a function of the variables b/B and B/D for constant velocity

	$b/B=$ 0.01	0.02	0.03	0.05	0.1	0.2	0.3	0.4	0.5
$B/D=$ 50	5.84	5.39	5.12	4.73	4.08	3.10	2.34	1.71	1.19
40	5.08	4.63	4.36	4.00	3.42	2.57	1.97	1.41	0.978
30	4.33	3.88	3.62	3.28	2.76	2.05	1.53	1.12	0.772
20	3.62	3.17	2.91	2.59	2.13	1.54	1.14	0.822	0.568
10	3.00	2.56	2.31	1.99	1.56	1.06	0.767	0.548	0.378
5	2.76	2.32	2.07	1.75	1.33	0.869	0.601	0.431	0.295
0	2.70	2.26	2.01	1.69	1.27	0.816	0.567	0.397	0.271
constant pressure for $B/D = 0$									
0	2.65	2.20	1.94	1.62	1.18	0.748	0.503	0.339	0.220

D has disappeared out of the end correction, suggesting that it should be possible to obtain this result with LAMB's theory as the starting point. This is indeed the case. In his "Hydrodynamics" [8] LAMB gives that, if an acoustic wave is impinging in the negative x direction normally upon a periodic arrangement of infinitely long slits in an infinitely thin screen, the acoustic potential Φ is given by (see Fig. 6)

$$\Phi=\exp(\mathrm{j}kx)+\exp(-\mathrm{j}kx)+\chi \qquad \text{if } x>0,$$

$$\Phi=\chi' \qquad \text{if } x<0.$$

Herein is

$$\chi=B_0\exp(-\mathrm{j}kx)+\sum_1^\infty B_n\exp(-\mathrm{j}k_nx)\cos b_ny,$$

$$\chi'=-B_0\exp(\mathrm{j}kx)-\sum_1^\infty B_n\exp(\mathrm{j}k_nx)\cos b_ny.$$

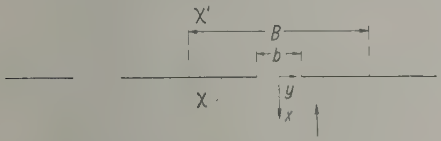

Fig. 6. To LAMB's problem.

At a distance great with respect to the wavelength the term under the summation sign can be neglected and we find that the amplitude of the reflected wave is $1+B_0$, whereas the amplitude of the impinging wave is 1. An expression for B_0 can directly be taken from LAMB

$$B_0=-1/(1+\mathrm{j}kL) \text{ with } L=\frac{B}{\pi}\ln\operatorname{cosec}\frac{\pi}{2}\frac{b}{B}.$$

The complex reflection coefficient

$$r=1+B_0=\mathrm{j}kL/(1+\mathrm{j}kL).$$

With the aid of $r=(z-\rho c)/(z+\rho c)$, where z is the specific acoustic impedance of the panel, we find easily $z=\rho c+2\mathrm{j}\omega\rho L$.

In our symbols this equation runs (see (18) for $d=0$)

$$z=\rho c+\mathrm{j}\omega\rho B\left(\frac{l}{b}\right)$$

or

$$l=\frac{2}{\pi}b\ln\operatorname{cosec}\frac{\pi}{2}\frac{b}{B}$$

the same expression that we found above.

8. Experimental verification of theory

Experiments have been carried out with a slit resonator of dimensions $d=4$ mm, $b=7.28$ mm, $B=228$ mm, $D=$ variable from 7.3 to 72.8 mm. An interferometer tube with a square cross section of 0.228×0.228 m^2 was used. It was closed by a completely reflecting heavy iron plate (15 mm thick). A metal sheet of 4 mm thickness was inserted in the tube at a variable distance ($D=7.3$ to 72.8 mm) in front of this rigid plate. The 4 mm thick sheet consisted of two rectangular halves leaving a slit of 7.28 mm breadth between them. Owing to symmetry this set up behaves like a system of infinitely long slits at 228 mm mutual distance. The resonance frequency has been measured on the one hand, the criterion for resonance being the vanishing of the imaginary part in the acoustical impedance, and calculated on the other hand (see Table II). For comparison the theoretical results, based on the formula of INGERSLEV-NIELSEN [6] are also included in the table. The agreement between the authors' theory and experiment is within the experimental error. That the values computed with INGERSLEV-NIELSEN's formula differ much more from experiment than ours is not surprising, since their formula is meant for the case of one single slit.

Table II

Measured and computed resonance frequency in Hz of a few slit resonators with $d=4$ mm, $b=7.28$ mm, $B=228$ mm.

D [mm]	Resonance frequencies according to			
	measurements	authors' theory const. velocity	authors' theory const. pressure	single slit theory
72.8	263	258	262	213
54.6	320	298	302	251
36.5	377	361	366	312
18.4	494	484	489	460
7.3	625	644	650	772

9. The design of resonators

If a panel is to be designed we are free in the choice of the resonance frequency, the absorption coefficient at resonance and the curve width of the absorption peak, the latter being defined as the number of octaves within which the absorption coefficient exceeds 50% of the value at resonance.

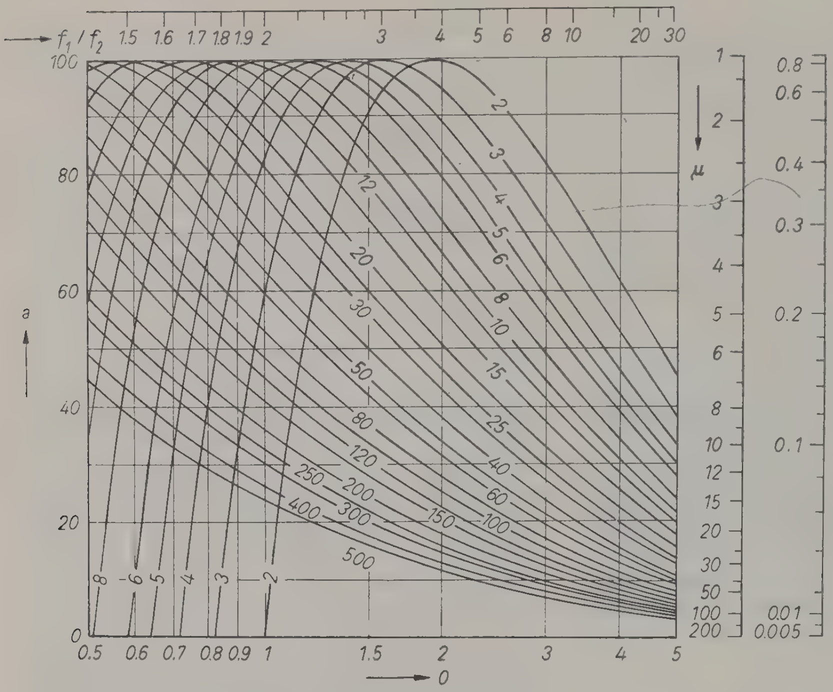

Fig. 7. Graph for finding the value $1/KD$ of a resonator from the requirements a) the absorption coefficient a at resonance and b) the number of octaves O for which the absorption coefficient exceeds $a/2$ (alternative for b: the ratio of the frequencies f_2 and f_1, for which the absorption should be $a/2$). The relative resistance μ is also read from the graph. Two values of O can be found for any pair of values a and $1/KD$. The lower value of O corresponds to the lower value of μ.

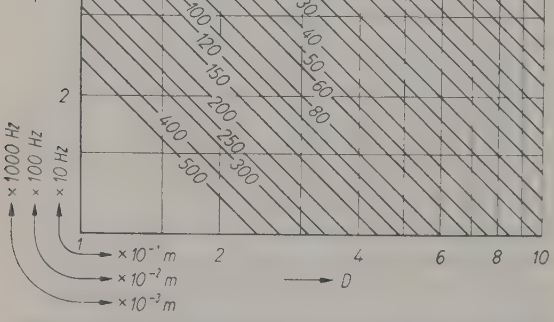

Fig. 8. Graph for computing D from the desired resonance frequency $f_{res.}$ and the quantity $1/KD$ (found from Fig. 7).

In order to treat this design problem along lines which we are acquainted with from the design of perforated panels with circular holes we rewrite eq. (18) in the generally used and approximate form

$$z = j\omega \frac{\rho}{K} + r + \frac{\varkappa p_0}{j\omega D}. \quad (21)$$

The stiffness term has been approximated in the usual way (eq. 17); furthermore we put for brevity

$$\frac{1}{K} = B\left(\frac{d}{b} + \frac{l}{b}\right)$$

and finally we introduced a resistive term r to allow for energy losses that are incidentally present or which have been introduced on purpose. The quantity K is normally called the conductivity per unit surface of the perforated system. For circularly perforated panels Zwikker and Kosten [1] gave a graph yielding the values of $D/\lambda_{res.}$ and $K\lambda_{res.}$ for any given set of numerical values of the absorption coefficient at resonance a, and the number of octaves O for which the absorption coefficient exceeds $a/2$. This graph can also be used for the design of slit resonators since the basic formula is identical. The graph is reproduced in Fig. 7, now giving $1/KD$ for any set a, O. At resonance the absorption coefficient only depends upon the resistive term r (see eq. (21)); the relation between a and $\mu = r/\rho c$ can be seen in Fig. 7. For the computation of $1/KD$ two of the three requirements have been used (a and O). The value D can now easily be derived from this value of $1/KD$ and the third requirement $f_{res.}$. For this purpose an equation is used that we obtain from eq. (18), with the aid of the definition of K

$$\frac{\cot(\omega_{res.} D/c)}{\omega_{res.} D/c} = \frac{1}{KD}; \quad (22)$$

see Fig. 8 representing this relation.

The problem now is to obtain a resonator construction with the desired values of $1/KD$ and D.

For slit resonators we have

$$\frac{1}{KD} = \frac{B}{D}\left(\frac{d}{b} + \frac{l}{b}\right) = \frac{B}{b}\frac{d}{D} + \frac{B}{D}\frac{l}{b}. \quad (23)$$

The value of $1/KD$ is a known function of the parameters B/D, b/B, d/D which is given graphically

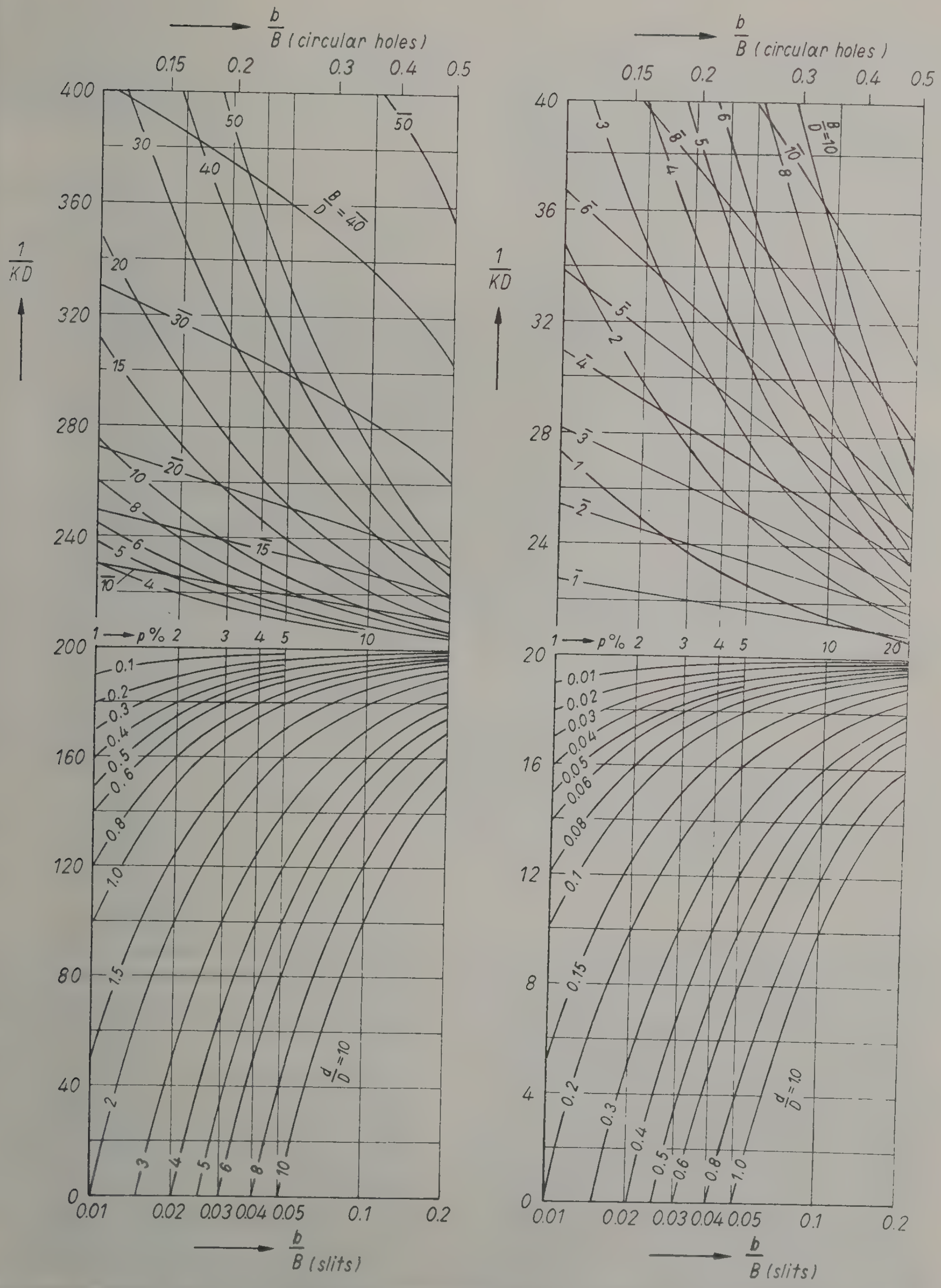

ig. 9. Design chart for resonators with slits or circular holes. Suitable dimensions of the resonator can be read from the graph for given values of $1/KD$ (from Fig. 7) and D (from Fig. 8) (see numerical example at the end of the publication).

in Fig. 9 for the case of constant velocity in the slit (B/D values with a bar). The numerical value of $1/KD$ is the vertical distance between a point with values b/B, B/D in the upper part of the figure and a point with values b/B, d/D in the lower part. This vertical distance is measured numerically with the $1/KD$-scale along the ordinate axis (see the numerical example later).

For resonators with circular holes an analogous equation can be derived with the aid of work done by NIELSEN [3]. If the holes are assumed to constitute a simple square lattice of period B and the diameter of the holes are labelled b, whereas d and D have the same meaning as above one finds

$$\frac{1}{KD} = \frac{4}{\pi}\,\frac{B^2}{b^2}\,\frac{d}{D} + \frac{4}{\pi}\,\frac{B}{b}\,\frac{B}{D}\,\mathrm{f}\left(\frac{b}{B}\right). \qquad (24)$$

The same combination of variables B/D, b/B, d/D can be seen in this equation, whereas the function f is given in a table by NIELSEN (ref. [3], pag. 25). The graph of this relation is also given in Fig. 9 (B/D values without a bar).

Only the upper parts of the graphs are different in both cases. The lower parts correspond to the first terms of the right hand members of eq. (23) and eq. (24) respectively. Introducing the perforation degree p, both terms are readily seen to be equal to $\frac{1}{p} \cdot \frac{d}{D}$, i. e., the contribution to $1/KD$ owing to these terms only depends upon the perforation degree (abscisa in the middle of the figures) and the value of d/D (values indicated along the curves in the lower part of the figures). The relation between p and b/B is expressed in Fig. 9 by adding a b/B-scale for circular hole perforation on top of the figure and a similar scale for slit perforation at the bottom.

One sees at a glance from Fig. 9 that, if two panels are compared, with holes and slits respectively, with identical degree of perforation p and identical ratio B/D, the $1/KD$-value for the slit panel is smaller than for the panel with holes for all practical dimensions, i. e., the slit panel is acoustically speaking the better one. It can be shown that the reverse is true, however, if two panels are compared with identical p and b/D. So if the holes in a panel are gathered in order to arrange them in the form of long slits the acoustic quality of the panel is impaired.

If one now desires to design a resonator for a certain resonance frequency ($f_{res.}$) with an absorption coefficient at resonance (a) and a number of octaves (O) the procedure is as follows: take from Fig. 7 the value of $1/KD$ and μ for the wanted a and O. Enter with this value of $1/KD$ Fig. 8 and find the depth D of the resonator for the wanted resonance frequency. Then a choice has to be made whether slits or circular holes should be used. Finally we enter Fig. 9 again with the value of $1/KD$, keeping in mind the value for D that was already found and read from the graph all desired data: B, b, d.

Example:

Requirements: $a_{res.} = 60\%$, a exceed 30% in two octaves ($O = 2$) around $f_{res.} = 500$ Hz.

Design: Fig. 7 yields $1/KD = 13$. Fig. 8 yields $D = 3 \times 10^{-2}$ m $= 3$ cm. Enter Fig. 9 with $1/KD = 13$ and $D = 0.03$. The value $1/KD = 13$, as read from the ordinate axis of Fig. 9, is marked by two points on a slip of paper. This is moved, remaining parallel to itself and the ordinate axis, in horizontal and vertical direction until the two marks indicate a sympathic design. The lower mark is bound to remain during this translation in the lower half of the figure and indicates d/D, e. g. $d/D = 0.1$, i. e. $d = 3$ mm since $D = 3$ cm. The upper mark is bound to remain in the upper half and indicates B/D. Two systems of curves are presented. Numerical values of B/D with a bar (e. g. $\overline{3}$) relate to slit absorbers, the unbarred values to normal circular perforation. In our case choosing $p = 2\%$ (= the percentage perforation; see abscisa-scale in the middle of the figure) a suitable pair of dimensions for slit absorbers is: $B/D = \overline{3.5}$, i. e. $B = 10$ cm; $b/B = 0.02$ (see bottom of figure), i. e. $b = 2$ mm. A combination of dimensions for circular holes and the same degree of perforation is found to be: $B/D = 1.6$, i. e. $B = 5$ cm; $b/B = 0.16$, i. e. $b = 8$ mm.

(Received 3rd May, 1951.)

References

[1] ZWIKKER, C. and KOSTEN, C. W., Sound absorbing materials. Elsevier, Amsterdam 1949.

[2] Lord RAYLEIGH, The theory of sound, Vol. II, p. 170, Macmillan, London 1929.

[3] NIELSEN, A. K., Acoustic resonators of circular cross section and with axial symmetry. Trans. Danish Acad. tech. Sci. 1949 No. 10.

[4] PEDERSEN, P. O., Lydtekniske Undersøgelser. Ingen-Vidensk. Skr. 1940 no. 5.
See also:
INGERSLEV, F., Akustik, A-S Dansk Ingeniørsforenings Forlag, København 1949;
JORDAN, V. L., J. acoust. Soc. Amer. **19** [1947], 976.
BRÜEL, P. V., First Summer Symposium of the Acoustic Group 1947. Resonant absorbers and reverberation. Published by the Physical Society London (1949) p. 10—23.

[5] INGÅRD, U., On the radiation of sound into a circular tube. Trans. Chalmers Univ. Tech., Gothenburg 1948, no. 70.; J. acoust. Soc. Amer. **20** [1948], 665.

[6] INGERSLEV, F. and NIELSEN, A. K., On the transmission of sound through small apertures and narrow slits. IngenVidensk. Skr. 1944, no. 5, p. 31.

[7] LAMB, H., Proc. math. Soc. London **29** [1898], 523.

[8] LAMB, H., Hydrodynamics, Ed. VI, p. 533 University Press, Cambridge 1932.

THE PRESSURE AND FIELD CALIBRATION OF MICROPHONES

by A. J. KING, D. Sc., M. I. E. E., F. Inst. P. and C. R. MAGUIRE, B. Sc., A. M. I. E. E.

(Metropolitan-Vickers, Manchester)

Summary

The paper deals with the calibration of microphones in the frequency range up to 20 kc/s. A description is given of the pressure calibration of condenser microphones in resonant tubes using Rayleigh discs for velocity measurement. The diffraction ratio is then determined using a Rayleigh disc in a lined cabinet and using a probe tube microphone in the same cabinet and also in a larger test room. The results are compared with the increase in pressure, due to the presence of the microphone, at specific points on the microphone diaphragm. The condenser microphones so calibrated may then be used to obtain the free field calibration of other microphones.

Sommaire

Etalonnage des microphones pour la bande de fréquences jusqu'aux 20 kHz. On décrit l'étalonnage dans un champ de pression des microphones condensateurs montés dans des tubes résonnants, la mesure de la vitesse s'effectuant au moyen de disques de Rayleigh. On détermine le rapport de diffraction dans une petite chambre insonore en se servant d'un disque de Rayleigh, ainsi que d'un microphone à sonde tubulaire dans la même chambre et puis dans une chambre d'essai de plus grandes dimensions. Les résultats sont comparés à l'augmentation de la pression sur certains points de la membrane du microphone par suite de la présence du microphone. Un tel microphone condensateur étalonné peut être employé pour l'étalonnage à l'air libre d'autres microphones.

Zusammenfassung

Die vorliegende Arbeit behandelt die Eichung von Mikrophonen im Frequenzbereich bis 20 kHz. Es wird die Druckeichung von Kondensatormikrophonen im Resonanzrohr beschrieben. Die Schallschnelle wird dabei mit einer Rayleighscheibe gemessen. Alsdann wird der Beugungseffekt bestimmt, und zwar 1. mit Hilfe der Rayleighscheibe in einem schallgedämpften Raum, 2. mit einem Sondenmikrophon im schallgedämpften Raum und 3. mit dem Sondenmikrophon in einem größeren Versuchsraum. Die Ergebnisse dieser Messungen werden verglichen mit der durch die Anwesenheit des Mikrophons hervorgerufenen Druckerhöhung an bestimmten Stellen der Mikrophonmembran. Ein auf diese Weise geeichtes Mikrophon kann zur Feldeichung anderer Mikrophone benutzt werden.

1. Introduction

On the occasions when it is necessary to measure the strength of a sound field it is usually the oscillatory pressure in free space which is required rather than the other attributes of a sound wave. This is probably due to the importance of the ear and its response to sound pressure. It is possible, in a simple progressive sound wave, to relate to each other the various attributes, pressure, velocity, amplitude and intensity, but in general it is desirable to have a ready method of determining sound pressure in a free field as directly as possible in absolute units. Few methods of measuring acoustic pressure directly in absolute units, especially in free space, are available and they are not very suitable as reference standards, e.g. methods depending on the change in refractive index of light waves with pressure, on radiation pressure associated with reflection [1] and on the voltages developed by piezoelectricity [2] and magnetostriction. The indirect method usually adopted is to measure the sound pressure by a reliable microphone and to calibrate this in absolute units in a known sound field. Two methods which have been used for generating known pressures or forces on a microphone diaphragm are by a thermophone [3] and by providing electrostatic forces to equal the acoustic forces [4] but neither is entirely satisfactory as a standard. It, therefore, became necessary to consider to what extent it would be permissible to measure one of the other attributes of an acoustic wave, such as amplitude or velocity, and rely on knowing the relation between the quantity measured and acoustic pressure. The methods of calibration described in this paper depend on the measurement of oscillatory particle velocity by the Rayleigh Disc, confirmed by measurements of oscillatory particle amplitude, and were developed in the Research Department of the company with which the authors are connected.

2. Discussion of the problem

To justify the substitution of a measurement of velocity or amplitude for that of pressure, it is necessary for the relation between pressure and the measured quantity to be a fundamental one not subject to appreciable uncertainty. This is the case in a sound wave remote from any disturbances, the relation between pressure and velocity being

$p = \rho c v$ where p = pressure in dynes/cm^2,
v = velocity in cm/s,
ρc = acoustic impedance of the medium,
= 42 CGS approx. for air,

and between pressure and amplitude

$p = 2\pi f a \rho c$ where f = frequency in c/s,
a = amplitude in cm.

However, there are many difficulties associated with measurement of oscillatory velocity or amplitude of air particles in free space. These difficulties are considered in detail later but those due to draughts can be reduced by working in a small enclosure and the additional ones due to uncertainty in the direction of incidence of the sound can be avoided by using a closed tube [1], [2], [5], [7] in which are excited longitudinal standing waves. Neglecting dissipation along the tube, the same relations between the p, v and a exist as in free space but the maximum movements occur a quarter of a wavelength along the tube from the maximum pressures.

In the past, the measurement of oscillatory particle velocity has relied mainly on König's formula for the torque developed on a Rayleigh disc in a moving air stream. ZERNOW [6], and BARNES and WEST [7] had shown that the formula was self consistent for thin, not too light discs of different sizes, and that it was approximately correct at low frequencies. MERRINGTON and OATLEY [8], on the other hand, found it was about 10% in error. This uncertainty has now been, for practical purposes, removed [9], [10], the residual uncertainty amounting only to less than 0.3 db. However, the calibration so obtained is the pressure calibration and does not take account of the diffraction of the sound wave by the microphone. This diffraction effect has been already investigated in several ways [11] but it is felt that the methods described in the present paper have some points of novelty.

It was obviously desirable that the microphone chosen for calibration as a standard should be stable in performance, should cause as little disturbance as possible to the free sound field and should lend itself to the method of calibration adopted. These requirements are satisfied by the condenser microphone shown in Fig. 1. The plane front avoids the cavity resonance associated with some types and provides good terminal reflection conditions for a resonant tube. Two sizes have been made, one exactly twice the other in all dimensions in order to simplify the determination of diffraction corrections as mentioned later.

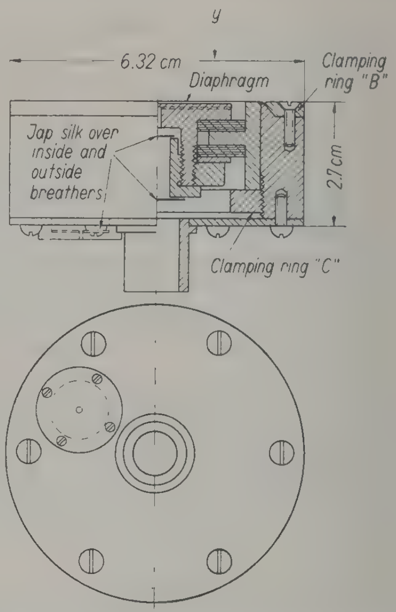

Fig. 1. Substandard condenser microphone. H.F. microphone is half size.

3. Pressure calibration by Rayleigh-disc-resonant-tube method

Arrangements which have been built up over the last 24 years for determining the pressure calibration of microphones [5] are illustrated in principle in Fig. 2. A closed tube in longitudinal resonance and containing an odd number of half waves, has maxima of pressure at the ends and of velocity at the middle. The microphone to be calibrated is therefore mounted at one end of the tube and a Rayleigh disc is suspended at the centre. The deflection of the disc on its calibrated suspension then provides a measure of the sound pressure acting on the microphone. The relation is:

$p = c\sqrt{\dfrac{1.5\rho T\delta\Theta}{r^3 \sin 2\Theta}}$ where p = sound pressure, dyne/cm^2,
ρ = air density, g/cm^3,

c = velocity of sound in air, cm/s,
T = control of suspension, dyne cm/radian,
Θ = angle between normal to disc and tube axis,
$\delta\Theta$ = angle turned by disc, radians,
r = radius of disc, cm.

If $\Theta=\pi/4$ and $\delta\Theta$ causes a scale deflection d [cm] at a distance of D [cm]

$$p=c\sqrt{\frac{0.75\,\rho\,T\,d}{r^3 D}}\ \text{approximately (corrected).}$$

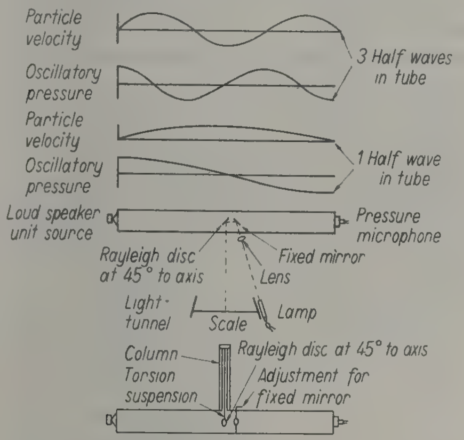

Fig. 2. Calibration of pressure microphones by Rayleigh-disc-resonant-tube method.

The frequency range from 25 c/s to 20 kc/s is covered by three tubes and the data relating to them are given in Table I. The reduction in tube diameter with increase in frequency, shown in this table, is necessary in order to ensure plane wave conditions in the tubes. Rayleigh [12] stated that if the diameter of the tube does not exceed 0.59 of the wavelength plane wave conditions are assured. However, it has been shown experimentally by comparison of tests in these three tubes and by explorations with a probe tube, that, as predicted by Rayleigh for a source symmetrical with respect to the axis, it is possible to work at frequencies up to twice this limit. In order to calibrate a microphone up to as high a frequency as possible, therefore, the tube diameter should be as small as possible and so should be made equal to that of the diaphragm, not that of the case. This was done for the medium and small tubes which were designed to test the two sizes of microphone shown in Fig. 1. These dimensions were chosen so that microphones could be calibrated up to approximately 10 and 20 kc/s respectively. The large tube was intended for testing various sizes of microphone, not always with plane diaphragms, so the large diameter ensured that a high proportion of the ends of the tube were plane, in the form of discs with holes to take particular sizes of microphones and source. The large tube uses a horn type loudspeaker unit as a source, but the medium and small tubes use electrostatic units with plane faces similar to the condenser microphones being calibrated. These electrostatic units are unpolarised and are driven at half the calibrating frequency so reducing pick-up troubles.

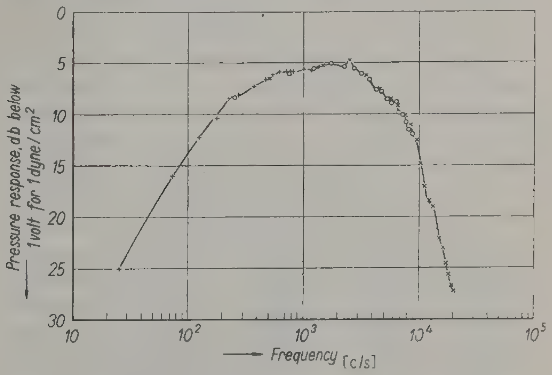

Fig. 3 Condenser microphone calibration in resonant tubes;
+ 696 cm tube,
○ 68 cm tube,
/ 34 cm tube.

Table I

Data on Rayleigh-disc-resonant-tubes

	large	medium	small
Tube length [cm]	696	68.0	34.0
Tube inside diameter [cm]	19.7	4.45	1.905
Frequency range [c/s]	25—1975	250—9250	500—20500
Rayleigh disc diameter [cm]	1.915	0.649	0.237_3
thickness [cm]	0.014	0.004	0.010
mass [g]	0.089	$3.3 \cdot 10^{-3}$	$1.1 \cdot 10^{-3}$
Suspension length [cm]	9.0	46	46
torque [dyne cm/radian]	$5.83 \cdot 10^{-3}$	$5.15 \cdot 10^{-4}$	$5.37 \cdot 10^{-4}$
Periodic time (approx.) [s]	12	5	
Effect on torque, walls [%]	0.7	1	0.8
disc thickness [%]	1.1	0.9	6
disc inertia [%]	—4.1	—3.2	—0.3
Pressure, r. m. s. [dynes/cm²] for deflection d [cm]	$5.59\sqrt{d}$	$9.05\sqrt{d}$	$41.3\sqrt{d}$

The lengths of the tubes correspond respectively to half a wavelength of their fundamental frequencies as shown in Fig. 2 and Table I. This table also gives the corrections for the Rayleigh disc readings necessitated by the proximity of the tube walls, the thickness of the disc, and its finite inertia. The suitability of these corrections has been discussed elsewhere [9].

The larger standard microphone has been calibrated in the large and medium tubes while the smaller microphone has been calibrated in all three tubes. The agreement between the three tubes is illustrated by Fig. 3. It is seen that over the frequency bands where the tubes overlap the agreement is within 2%, the limit of experimental error.

4. Field calibration

a) Rayleigh disc in lined test cabinet

The pressure calibration described differs from the free field calibration by the diffraction ratio, which with high impedance microphones will depend only on their external dimensions. This section describes a method of determining this ratio by direct calibration of the microphone in free field against the Rayleigh disc. Since the Rayleigh disc is sensitive to unidirectional as well as to oscillatory flow precautions are necessary to reduce spurious deflections due to casual air currents.

The difficulty of preventing casual air currents of sufficient magnitude to affect the Rayleigh disc readings increases with the size of the room in which the measurements are made so a small lined cabinet was constructed. This cabinet, approximately 1.3 m³, was closed by a well fitting door and lined with 15 cm cotton waste to reduce reflection from the walls.

The Rayleigh disc was suspended from a brass tube which passed through the centre of the top of the cabinet in such a way that the Rayleigh disc was normally suspended at the centre of the cabinet but could be raised to allow the microphone to take its place, without opening the door. The microphone was mounted on a carriage sliding on rods near the floor of the cabinet, so that it could be moved into the central position previously occupied by the Rayleigh disc or to a remote position against one wall. The sound source consisted of a 20 W moving coil unit mounted externally, and feeding into the cabinet through a bakelite tube 0.6 m long by approx. 18 mm inside diameter, which passed through the centre of one vertical edge of the cabinet and pointed towards its centre. This sound source was mounted on guides so that the distance from its open end to the centre of the cabinet could be varied. The substitution of the microphone for the Rayleigh disc and vice versa as well as the change in source position could be effected without opening the door of the cabinet and disturbing the stable air conditions inside. The oscillatory velocity was then calculated from the constants of the disc and suspension and the deflection of a spot of light reflected from a concave mirror on the disc to a suitable scale inserted in the front wall of the cabinet.

From the results obtained with different source positions in this cabinet and the pressure calibration obtained in the resonant tubes, diffraction ratios were calculated and are shown as points in Fig. 4. These values have been corrected for the difference between the diffraction ratio in a spherical field and that in a plane progressive wave [13].

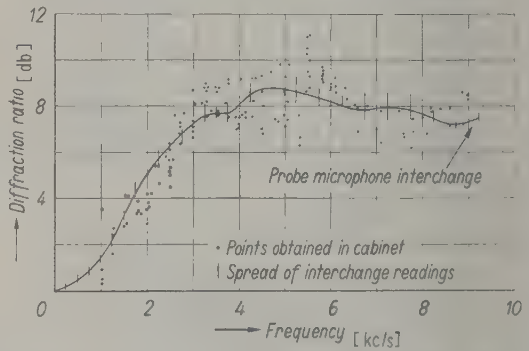

Fig. 4. Diffraction ratio as determined by Rayleigh disc in cabinet and probe microphone in test room.

The spread of the results at a fixed frequency but at different distances from microphone to source often exceeded 2 db, whereas the difference between repeated readings at the same distance seldom exceeded 0.2 db. This is a larger spread of results than would be expected from the known variations in the field in the neighbourhood of the microphone, or from uncertainties in the corrections which have been applied to correct for the curvature of the wave front.

It is felt that the spread is to some extent due to changes in effective direction of the waves arriving at the Rayleigh disc due to changes in the sound field in the cabinet with movement of the source.

b) Probe tube microphone in cabinet

From experience with the Rayleigh disc in the cabinet it was expected that a pressure measuring device would yield better results than one affected by direction. A probe tube microphone [14] was therefore used, in which the microphone was situated outside the cabinet. The tube was 6 mm external diameter and so had little diffraction ratio over the desired frequency range. The calibration of the probe tube microphone was carried out in the Rayleigh disc tubes as described later (section c), but the field calibration of the substandard microphone at a fixed frequency, but with different source to microphone distances still varied by as much as 2 db indicating that the field conditions were not sufficiently good. Improvements in the coefficient of absorption of the linings of the cabinet, in the frequency range involved, failed to produce any significant improvement in the spread of the results.

c) Probe tube microphone in test room

Since the diffraction ratio as measured in the cabinet was a function of the distance of the microphone from the source and since a further increase in this distance was not possible in the cabinet without approaching undesirably close to the absorbent walls it was decided to continue the work in a test room [14] (7.2 m × 7.2 m × 3.9 m high) which is lined with 15 cm cotton waste backed with a 15 cm air gap. The sound source consisted of a 20 W loudspeaker unit with a 12.5 mm diameter opening, which projected through the lining of the test room in one corner at 1.65 m above floor level. The uniformity of the field in the calibrating region was improved by breaking up the smooth surfaces in the vicinity of the source with loose irregular bunches of cotton waste. Field explorations in three directions, mutually at right angles, were carried out at all frequencies at which measurements were made and none of the variations exceeded 1 db in the region of the microphone. Typical field decay curves are shown in Fig. 5.

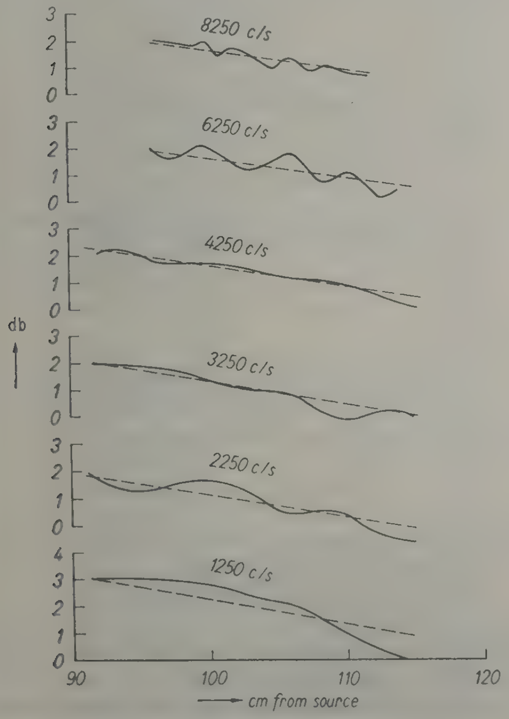

Fig. 5. Field distribution in test room.

In order to measure the free field sound pressure a probe tube microphone had to be developed which could be introduced into the measuring field without appreciable distortion and which would be sensitive only to pressure at its open end. The tube was of copper 3 mm inner diameter, 6 mm outer diameter and 0.8 m long with sufficient absorption in the form of wool at each end to reduce the variations in sensitivity due to resonances in the tube to less than 2%. The microphone, Fig. 1, was enclosed in a 12.5 mm thick brass cylinder with a massive front and the whole flexibly supported in a second massive cylinder, see Fig. 6. The double skin gave an attenuation greater than 40 db between sound entering by the open end of the probe tube and sound passing into the microphone by other paths. This was measured by plugging the open end of the tube with a suitable cap and noting the reduction in output.

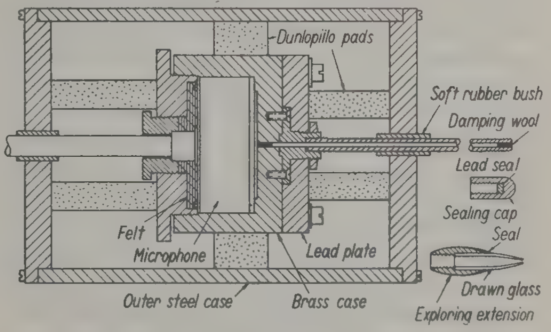

Fig. 6. Probe microphone in steel case.

As the probe tube microphone was to be used in the sound field it was essential that the disturbance of the sound field at the mouth of the probe by reflections from the casing should be small. The casing was accordingly enveloped in an ellipsoid of cotton waste of major and minor axes 55 and 25 cm respectively. In this condition the maximum change in sound field at the probe mouth due to the body as checked by bringing up a similar ellipsoid was 0.2 db at 1000 c/s and less than 0.1 db at all other frequencies used.

The probe tube microphone was calibrated [14] by inserting it through a resilient bush in one end of a Rayleigh disc tube to such a distance that the opening was at a pressure maximum. Readings with the probe mouth flush with the end piston were the same as those at other pressure maxima. Exploration of the sound field across the probe mouth with a second probe microphone indicated that the disturbance of the sound field in the resonant tube due to the presence of the probe tube was less than 1% up to 8000 c/s.

The technique adopted for the free field calibration of a substandard microphone was to suspend it and the probe tube microphone in the test room in such a manner that, when the substandard was removed, the open end of the probe tube moved into the position previously occupied by the centre of its diaphragm. At each frequency readings were taken at five or more microphone positions over a total distance of approximately twice the wavelength except at low frequencies when the maximum change was limited to about 25 cm. The spreads of the results of these tests are shown by the vertical lines in Fig. 4, the curve being drawn through the mean values. These values have been corrected for the diffraction ratio of the probe tube which amounts to 1.2 db at 9000 c/s.

To provide a check on the diffraction ratio curve obtained by this interchange method, direct measurements were made of the increase in pressure in front of the microphone diaphragm. This was done by bringing the condenser microphone up to a probe microphone fitted with a small bore tip which remained stationary in the sound field. Two sets of readings were taken, at each frequency and over the previous range of source to microphone distances, at positions corresponding to the centre of the diaphragm and to the edge of the back plate. The results of these measurements are shown in Fig. 7 together with the diffraction ratio curve as obtained by the interchange method. A check with a second probe tube microphone inserted from the rear through the centre of a dummy condenser microphone showed that the presence of the probe tube did not alter the pressure at the centre of the microphone by more than 0.1 db at any frequency up to 7000 c/s or more than 0.5 db up to 9500 c/s.

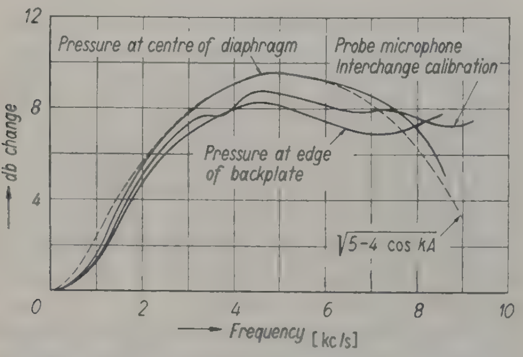

Fig. 7. Pressure change due to diffraction at the surface of the microphone.

Measurements of the sound pressure in the region of the microphone were made using the probe microphone and typical curves are shown in Fig. 8 and 9. These curves show that the diffraction pattern round the microphone produces considerable changes over distances several times the microphone diameter while the change in front of the microphone is 0.5 db at a distance of 80 cm when the frequency is 5000 c/s.

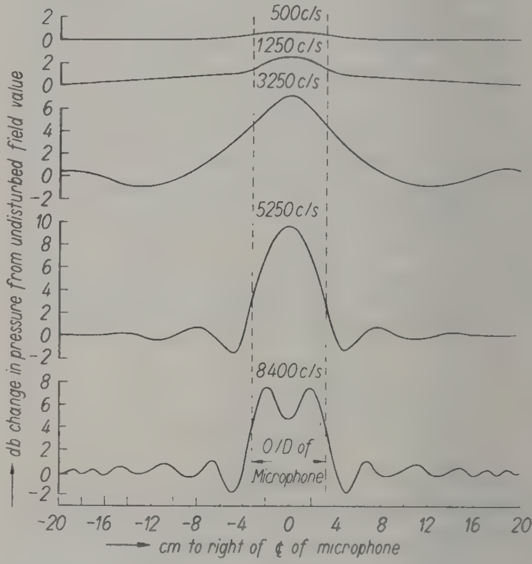

Fig. 8. Change in pressure in plane of microphone diaphragm due to diffraction by microphone body.

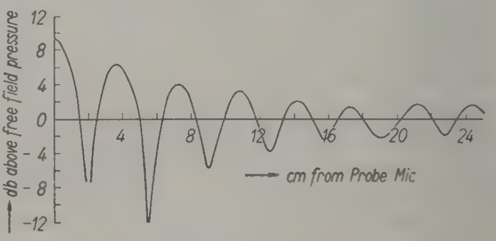

Fig. 9. Change in pressure at a point as microphone is moved away; frequency = 5000 c/s,
total variation at 60 cm = 0.7 db,
total variation at 85 cm = 0.4 db.

d) Comparison of results of different methods

Although the results obtained with the Rayleigh disc in the lined cabinet have a large spread they are in good general agreement with the curve obtained using the probe interchange method except in the region of 2500 c/s (see Fig. 4). Here, however, the difference between the pressure increase at the centre of the diaphragm and that at the edge of the backplate is only about 0.7 db (see Fig. 7), and the curve of diffraction ratio, obtained by the interchange method, lies midway between. It is unlikely that these concordant results are in error and it is, therefore, probable that the results in the cabinet are in error in this region.

The spread of the results obtained with the probe microphone in the test room, as shown by the vertical lines in Fig. 4, was considerably less than the spread using the Rayleigh disc in the lined cabinet although more readings were involved and the variation of source to microphone distance larger. The reduced spread of the results was probably due not only to the improved field conditions in the large test room but also to the freedom of the probe from any critical dependence on direction, as compared with the marked directional response of the Rayleigh disc. The mean diffraction curve obtained by these methods is compared, in Fig 7, with two curves which show the change in pressure, at different positions on the front face of the microphone, due to the disturbance of the sound field by the microphone. Good agreement is shown up to 6500 c/s except in the region of 3700 c/s where a marked dip occurs in the interchange curve. Measurements of diffraction ratio at the rear of the microphone indicated that this dip was critically dependent on the length of the microphone, and that this length effect could alter the diffraction ratio by ± 0.8 db in this frequency region.

The increase of pressure at the centre of a flat infinitely thin circular disc due to reflection of sound from its front face for the case of normal incidence may be expressed as [13]

$$\frac{p_1}{p_0} = \sqrt{5 - 4 \cos k A}$$

where p_1 = pressure at centre of disc,
p_0 = pressure in absence of microphone,
A = radius of disc,
k = wavelength constant $= 2\pi/\lambda$,
λ = wavelength.

This has been evaluated for a disc of diameter 6.31 cm and plotted as a dotted curve in Fig. 7 where it is in good agreement with the pressure change at the centre of the microphone over the frequency range covered. The expression for p_1/p_0 gives successive maxima when the diameter is an odd multiple of the wavelength and minima at even multiples, corresponding to a pressure node at the centre and an increased pressure at one or more annular rings between the centre and the outside edge. This effect is demonstrated in Fig. 7 where the pressure at the edge of the backplate exceeds that at the centre by 2 db at 8500 c/s.

These results were obtained on two substandard microphones of the same dimensions, see Fig. 1. Although the pressure calibrations differed at certain frequencies by 25% no significant difference in diffraction ratio could be detected at any frequency in the range covered. The increase in pressure at the surface of each agreed with that obtained with a solid brass dummy of the same dimensions, implying that the impedance of the diaphragm is very high and that changes in its tension will not affect the diffraction ratio.

To extend the range of calibration to 20 kc/s, it has been considered entirely justifiable to use the diffraction curve of Fig. 4 with a doubled frequency scale for the half size microphone of Fig. 1.

e) Interchange calibration of other microphones

The calibration of other microphones in terms of our calibrated laboratory condenser microphones is carried out by substitution in the test room referred to previously. The microphone to be calibrated and the standard are supported 1.5 m apart on a triangular wire frame so that, by operating controls in an adjacent room, each microphone in turn can be made to occupy the position in front of the source in the corner of the room where the probe measurements were carried out. The field uniformity there, see Fig. 5, is adequate for practical purposes so a straightforward calibration by substitution is a routine matter.

5. Conclusions

The technique described using the Rayleigh disc and König's formula enables the pressure and field calibrations of diaphragm type microphones to be determined with a consistency of 2%. Measurements of particle amplitude show that the absolute sensitivities do not differ by more than 3% from the values obtained as above. Routine calibrations of microphones of any type can be made by comparison with reliable laboratory standards which have not changed by 1 db in nearly 20 years.

Acknowledgements

The authors wish to acknowledge the help of several of the staff of the Research Department of Metropolitan-Vickers Electrical Co. Ltd., during the course of the investigation and of Mr. W. R. Cor-

FIELD, who carried out much of the experimental work while on the staff of the Acoustics Laboratory. They also express thanks to Sir Arthur P. M. FLEMING, C. B. E., D. Eng., Director of Research and Education, and Mr. B. G. CHURCHER, M. Sc., M. I. E. E., Manager of Research Department, for permission to publish this paper.

(Received 25th January, 1951.)

References

[1] CHURCHER, B. G. and King, A. J., J. Inst. electr. Engrs. **68** [1930], 97.
[2] COOK, R. K., J. Res. nat. Bur. Stand., Wash. **25** [1940], 489.
[3] WENTE, E. C., Phys. Rev. **19** [1922], 333.
[4] GERLACH, E., Wiss. Veröff. Siemens **3** [1923], 139.
[5] KING, A. J., Metrop.-Vick. Gaz. September [1947], 153.
[6] ZERNOW, W., Ann. Phys. Lpz. (4) **26** [1908], 79.
[7] BARNES, E. J. and West, W., J. Inst. electr. Engrs. **65** [1927], 871.
[8] MERRINGTON, A. C. and OATLEY, C. W., Proc. Roy. Soc. (London) A **171** [1939], 505.
[9] SCOTT, R. A., Proc. Roy. Soc. (London) A **183** [1945], 296.
[10] WEST, W., Proc. phys. Soc. B **62** [1949], 437.
[11] BALLANTINE, S., J. acoust. Soc. Amer. **3** [1932], 319.
[12] Lord RAYLEIGH, Theory of sound II, 2nd ed. p. 161.
[13] SIVIAN, L. J. and O'NEIL, H. T., J. acoust. Soc. Amer. **3** [1932], 483.
[14] KING, A. J. and MAGUIRE, C. R., Nature (London) **141** [1938], 1016.

DIE SCHWINGUNG DER LUFTTEILCHEN IN DER NÄHE EINER SCHALLABSORBIERENDEN WAND

Von E. MEYER und R. W. KARMANN
(III. Physikalisches Institut der Universität Göttingen)

Zusammenfassung

Mit Hilfe suspendierter Teilchen wird die Schallfeldstruktur in der Nähe einer schallabsorbierenden Wand genauer untersucht. Dazu werden in einem Rohr mit quadratischem Querschnitt fortschreitende Schallwellen der Frequenzen 100 . . . 500 Hz erzeugt, wobei in die untere Rohrwand nacheinander verschiedene schallabsorbierende Anordnungen eingesetzt werden, deren Impedanzen aus Messungen im KUNDTschen Rohr bekannt sind. Die Bewegung der suspendierten Teilchen erfolgt in der Regel in einer elliptischen Bahn, deren große Achse gegen die Schallschluckfläche geneigt ist. Die Bahn wird mittels indirekter Beleuchtung sichtbar gemacht und photographiert.

Nach der MORSEschen Theorie ist das Verhältnis Längsschnelle zu Querschnelle der Teilchen im Rohr $\overline{C}(z)$ durch den Ausdruck

$$C(z) = \frac{\rho\overline{c}\,\mathrm{tg}\,\overline{\gamma}z}{\overline{W}\,\mathrm{tg}\,\overline{\gamma}H}$$

gegeben, wobei $\rho\overline{c}$ den Wellenwiderstand und $\overline{\gamma}$ die Fortpflanzungskonstante in Rohrrichtung, W den Wandwiderstand des Absorptionsmaterials sowie z bzw. H den Abstand des Meßpunktes bzw. der schallabsorbierenden Wand von der gegenüberliegenden schallharten Wand bedeuten. Aus $\overline{C}(z)$ folgen das Achsenverhältnis der elliptischen Bahn sowie der Neigungswinkel gegen die Rohrachse.

Die Meßergebnisse an verschiedenen Schluckstoffen (30 cm dicke Glaswolleschicht, λ/4- bzw. λ/2-Resonatoren mit Wattedämpfung, Schlackenwollekeile als ρc-Abschluß) stehen mit den berechneten Werten in guter Übereinstimmung.

Summary

The sound field in a tube lined with absorbent material of known impedance is investigated with the aid of particles in suspension, for frequencies between 100 and 500 Hz. The particles follow an elliptical path. From the wall impedance the axes of the ellipse and their inclination to the axis of the tube are calculated, using the theory of MORSE. Theoretical and experimental results are in good agreement.

Sommaire

La structure du champ sonore au voisinage d'une paroi absorbante a été étudiée en photographiant des trajectoires elliptiques suivies par les particules en suspension dans un tube horizontal de section carrée, dans lequel on forme des ondes progressives (100 à 500 Hz). La paroi inférieure du tube est le matériau absorbant étudié. Du rapport des vitesses longitudinale et transversale des particules, fourni par la théorie de MORSE, on déduit le rapport des axes des trajectoires et leur inclinaison sur l'axe du tube. Les résultats expèrimentaux relatifs à différents matériaux (laine de verre), résonateurs en λ/2 ou λ/4 avec coton, sont en bon accord avec les valeurs calculées.

1. Einleitung

Es ist bekannt, daß eine Schallwelle, die sich längs einer absorbierenden Schicht ausbreitet, von dieser stark beeinflußt wird. Es tritt eine zusätzliche Schalldämpfung auf, auf die zuerst VON BÉKÉSY [1] hingewiesen hat und die im Falle des Publikums als eines porösen Absorbers praktisch eine beachtliche Rolle spielt. Außerdem wird die Wellennormale der fortschreitenden Welle zur schallabsorbierenden Fläche hin geneigt. Der letztgenannte Effekt wurde von MEYER und BUCHMANN [2] in einem Ultraschallfeld mit Hilfe einer Rayleighscheibe bestätigt; ähnliche Ergebnisse erhielten JANOWSKI und SPANDÖCK [3] mit Richtmikrophonen in einem schallgedämpften Raum.

Leichter zu übersehen sind die Verhältnisse, wenn man die Schallwelle in einem Rohr sich ausbreiten läßt, von dem z.B. eine oder mehrere Wände mit einem Schallschluckstoff ausgekleidet sind. Auch hier bekommt man wiederum eine starke Erhöhung der Ausbreitungsdämpfung und eine Veränderung der Phasengeschwindigkeit, abhängig von den Rohrdimensionen und von den Wandwiderständen des Schluckstoffes. Diese Fragen sind theoretisch von SIVIAN [4], von CREMER [5] und insbesondere von MORSE [6], der hierzu auch die rechnerischen Unterlagen geschaffen hat, behandelt worden; W. LIPPERT [7] hat in zahlreichen Versuchen eine gute Übereinstimmung mit der Theorie gefunden.

Die vorliegende Arbeit stellt insofern eine Ergänzung zu diesem Problemkreis dar, als die Bewegung der Luftteilchen an einer absorbierenden Wandfläche des Rohres berechnet und gemessen wird. Sind alle Wände des Rohres schallhart, erfolgt natürlich die Schwingung der Luftteilchen längs gerader Linien parallel zur Rohrachse, wobei die Amplitude in großer Nähe der Wand (akustische Grenzschicht) sehr klein, und schließlich, unmittelbar an der Wand, ganz zu Null wird. Wird nun eine Wandfläche mit einem Schallabsorptionsmaterial ausgekleidet, so liegt die Vermutung nahe, daß im allgemeinen elliptische Bahnen auftreten, deren Achsen zu der betreffenden Wandfläche hin geneigt sind. Auch hierfür werden, wie bei der Schalldämpfung und der Phasengeschwindigkeit, die Dimensionen des Rohres, speziell der Abstand des Luftteilchens von der Absorptionsfläche, sowie der Widerstand des Materials maßgebend sein.

2. Zur Theorie

Längs des Rohres von rechteckigem Querschnitt (Abb. 1) möge sich eine ebene, rein fortschreitende Welle ausbreiten. Der Rohrdurchmesser ist klein zur Wellenlänge, das Rohr ist durch eine keilförmige Schluckstoffanordnung mit dem Wellenwiderstand abgeschlossen. Bei allseitig harten Rohrwänden schwingen, wie bereits erwähnt, die Luftteilchen parallel zur Rohrachse, es tritt also eine reine Längsamplitude auf. Wird dagegen eine Rohrwand, z.B. der Boden des horizontal liegenden Rohres, durch ein absorbierendes Material vom akustischen Widerstand W ersetzt, dann durchläuft die Welle das Rohr mit der komplexen Phasengeschwindigkeit c, deren Betrag im allgemeinen kleiner als die Ausbreitungsgeschwindigkeit im freien Medium ist; das Rohr hat dann den Wellenwiderstand ρc. Damit tritt zu der Längsamplitude der Luftteilchen eine Queramplitude. Diese Queramplitude wird Null an der oberen, der Schluckstofffläche gegenüberliegenden harten Wandfläche. Direkt an der Schluckstoffoberfläche, $z = H$ (Abb. 1), gilt dagegen für das Verhältnis Queramplitude zu Längsamplitude die einfache Beziehung $C(H) = \frac{\rho c}{W}$.

Ist Φ das Geschwindigkeitspotential in dem Ausbreitungsraum, dann heißt die unter der Annahme sinusförmiger Schwingungen separierte Wellengleichung

$$\Delta \Phi + k^2 \Phi = 0, \tag{1}$$

wobei $k = \omega/c$, die Wellenzahl bei freier Ausbreitung ist.

Da es sich in x-Richtung um eine rein fortschreitende und gedämpfte, in der z-Richtung um eine stehende Welle handelt, lautet der Lösungsansatz:

$$\Phi = \left(A_1 \, e^{j\gamma z} + A_2 \, e^{-j\gamma z}\right) e^{-j(kx - \omega t)} \tag{2}$$

(γ Ausbreitungskonstante in z-Richtung und k Ausbreitungskonstante in x-Richtung).

Der Ansatz muß den beiden Randbedingungen genügen:

$$\left(v_z\right)_{z=0} = -\left(\frac{\partial\Phi}{\partial z}\right)_{z=0} = 0; \quad \left(\frac{p}{v_z}\right)_{z=H} = W, \tag{3}$$

wobei p der Schalldruck und v_z die Schnelle in z-Richtung sind.

Mit der ersten Bedingung erhält man als Lösung:

$$\Phi = \Phi_0 \cdot e^{-j(kx - \omega t)} \cdot \cos \gamma z. \tag{4}$$

Aus der zweiten Bedingung ergibt sich die Bestimmungsgleichung für γ:

$$\mathrm{tg}\, \gamma H = \frac{\omega \rho}{j \gamma W}. \tag{5}$$

Diese Gleichung hat für einen vorgegebenen Wandwiderstand W unendlich viele Lösungen für γ, die auf RIEMANNschen Blättern 1., 2., ... Ordnung liegen. Nur die Lösung 1. Ordnung interessiert in unserem Zusammenhang.

Mit der aus der Wellengleichung folgenden Beziehung

$$k^2 = \gamma^2 + k^2 \tag{6}$$

ist auch die Berechnung von k möglich.
Die numerische Ausrechnung von Gl. (5) und (6) in den verschiedenen Fällen wurde mit Hilfe der Diagramme von MORSE durchgeführt.

Das Verhältnis von Quer- zu Längsamplitude bzw. das Verhältnis der entsprechenden Schnellen läßt sich nun mittels Gl. (4) bilden:

$$\frac{v_z}{v_x} = \frac{\partial \Phi / \partial z}{\partial \Phi / \partial x}$$

$$= \frac{\gamma\, \mathrm{tg}\, \gamma z}{j k} = C(z) = C(z)\, e^{j\psi}, \tag{7}$$

dabei ist ψ die Phasendifferenz zwischen v_z und v_x. Man erhält also allgemein eine elliptische Teilchenbewegung.

Setzt man Gl. (5) in (7) ein und setzt $z = H$, so erhält man:

$$C(H) = \frac{\gamma\, \mathrm{tg}\, \gamma H}{j k} = \frac{\rho c}{W}, \tag{8}$$

eine Beziehung, die unmittelbar anschaulich ist und schon eingangs angeführt wurde.

Für das Amplitudenverhältnis in einer beliebigen Höhe z erhält man (Substitution des Faktors γ in Gl. (7) durch Gl. (8)):

$$C(z) = C(H) \cdot \frac{\mathrm{tg}\, \gamma z}{\mathrm{tg}\, \gamma H}. \tag{9}$$

Beim Übergang von einem Punkt auf der Schluckstofffläche (Höhe $z = H$) auf einen solchen in beliebiger Höhe z ist also das Transformationsglied $\mathrm{tg}\, \gamma z / \mathrm{tg}\, \gamma H$ maßgebend.

Zur Charakterisierung der elliptischen Schwingung dient gemäß Gl. (7) das Verhältnis der Amplituden $C(z) = |C(z)|$ sowie die Phasenverschiebung ψ zwischen v_x und v_z.

Aus meßtechnischen Gründen ist es zweckmäßiger, zwei andere Parameter zur Kennzeichnung zu wählen, nämlich die Neigung δ der großen Ellipsenachse gegen die Rohrachse und das Verhältnis der kleinen zur großen Ellipsenachse β/α. Der Zusammenhang zwischen den einzelnen Größen ist:

$$\begin{gathered} \mathrm{tg}\, 2\delta = \frac{2\, C(z) \cos\psi}{1 - C^2}, \\ \frac{\beta^2}{\alpha^2} = \frac{1 + C^2 - \sqrt{(1 - C^2)^2 + 4 C^2 \cdot \cos^2\psi}}{1 + C^2 + \sqrt{(1 - C^2)^2 + 4 C^2 \cdot \cos^2\psi}}. \end{gathered} \tag{10}$$

3. Meßmethode

Abb. 1 zeigt einen schematischen Schnitt durch die Versuchsapparatur. Die Schallamplituden in einem Rohr von rechteckigem Querschnitt, dessen seitliche Wände aus Kristallglasscheiben bestehen, werden durch kleine, in Luft suspendierte Teilchen sichtbar gemacht. Das Rohr ist auf der einen Seite mit einem Lautsprecher mit vorgeschalteter Druckkammer, auf der anderen Seite mit dem Wellenwiderstand abgeschlossen, der durch einen genügend langen Keil aus Schlackenwolle realisiert ist. Die Druckkammer dient zur Erhöhung der Schwingungsamplitude im Rohr. An der unteren Seite des rechteckigen Rohres wird der zu untersuchende akustische Widerstand angeschlossen.

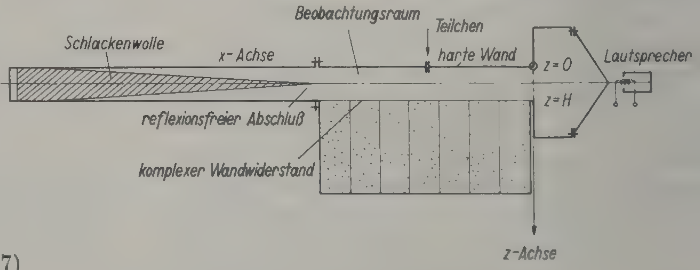

Abb. 1. Schnitt durch die Versuchsanordnung.

Als Stoff für die Teilchen wurde in dieser Arbeit $Mg_3(OH)_2Si_4O_{10}$ (Talkum) verwendet, der keinerlei Neigung zur Koagulation hatte und hinsichtlich der Teilchengröße so günstig lag, daß es der Bedingung der nahezu vollständigen Mitnahme (90%):

$$r^2 \cdot \nu = 10^{-6}\ \mathrm{cm^2\, s^{-1}}$$

(r = Radius des Teilchens; ν = Frequenz; Dichte der Teilchen = 2,7 g/cm³ angenommen) genügte.

Abb. 2 zeigt eine elektronenmikroskopische Aufnahme der verwendeten Teilchen[1]. Die Ausmessung ergibt, daß die Teilchen die Luftschwingung bis etwa 500 Hz nahezu vollständig mitmachen.

Abb. 2. Elektronenmikroskopische Aufnahme eines Schwebeteilchens.

Die in den Beobachtungsraum hineingeblasenen Teilchen werden durch Dunkelfeldbeleuchtung sichtbar gemacht. Der Strahlenverlauf ist in Abb. 3 dargestellt. Die Beobachtung erfolgt senkrecht zur Bildebene der Abb. 1. Das Licht der Bogenlampe wird durch einen lichtstarken Kondensor gesammelt und von der Zentralblende vor dem Beleuchtungsobjektiv teilweise abgefangen, so daß nur Licht von ringförmigem Querschnitt durch das Beleuchtungsobjektiv stark gebündelt die Teilchen sehr hell beleuchtet. Das abbildende Objektiv des Mikroskops steht im Schatten der Zentralblende.

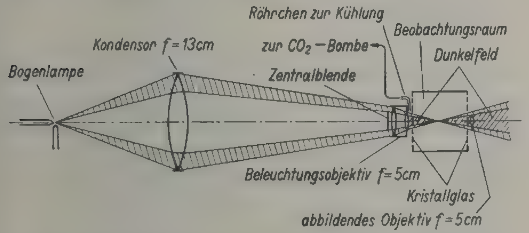

Abb. 3. Strahlenverlauf der optischen Einrichtung.

Besondere Vorsorge mußte zur Verhinderung von Konvektionsströmungen getroffen werden, die durch geringste Temperaturunterschiede hervorgerufen wurden. Die Erwärmung des Kristallglases durch teilweise Absorption des energiereichen Lichtbündels konnte stets für gewisse Zeit durch den JOULE-THOMSON-Effekt kompensiert werden, indem unter Druck stehende Kohlensäure sich über zwei dünne Röhrchen, die unmittelbar an der abzukühlenden Glasfläche endeten, auf Atmosphärendruck entspannte.

Zu Messungen wurde ausschließlich eine mikrophotographische Aufnahme mit 15facher Vergrößerung verwendet. Nach jeder Aufnahme mußte noch die Rohrachse als Bezugslinie auf dem Film mitphotographiert werden.

4. Versuchsmaterial

Folgende akustische Widerstände wurden u. a. untersucht:

1. Glaswolle in 30 cm Schichtdicke mit einer Stopfdichte von 80 kg/m³;
2. Ein System aus parallelen Röhren von 36,5 cm Länge, die mit einer Watteschicht von 1 cm Dicke eingangsseitig abgeschlossen sind (die Röhren sind am Ende hart abgeschlossen);
3. Abschluß mit dem Wellenwiderstand, der durch eine Schlackenwolle-Keilanordnung verwirklicht ist.

Bei allen Anordnungen ist eine Kassettierung vorgenommen, um eine Wellenausbreitung im Schluckstoff zu verhindern und die Wandimpedanz winkelunabhängig zu machen.

Die Impedanzen der Absorptionsanordnungen wurden im KUNDTschen Rohr gemessen. Das Ergebnis zeigt Abb. 4 in Form von Ortskurven; Real- und Imaginärwerte sind in ϱc-Einheiten aufgetragen, die Zahlen an den Kurven bedeuten Frequenzen in Hz.

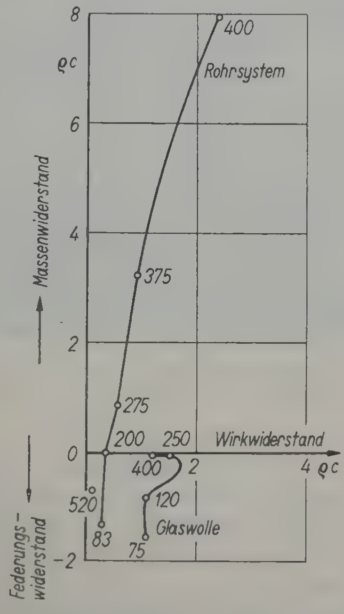

Abb. 4. Im KUNDTschen Rohr ermittelte Impedanzwerte der Versuchsmaterialien mit der Frequenz als Parameter.

---

[1] Für diese Aufnahmen sind wir Frl. KNOCH zu Dank verpflichtet.

Die nächsten Abbildungen sind Beispiele von Teilchenbewegungen. Abb. 5 zeigt zunächst die Teilchenschwingung bei hartem Abschluß und der Frequenz 120 Hz. Die Teilchen schwingen parallel zur Rohrachse und haben alle die gleiche Länge, die ein Maß für den Teilchenausschlag bzw. die Teilchenschnelle ist. In den Abb. 6, 7 und 8 sind Teilchenschwingungen für verschiedene Wandwiderstände in 5,5 cm Entfernung über der Schluckstoffoberfläche photographiert. Die horizontale Linie ist die Rohrachse als Bezugslinie.

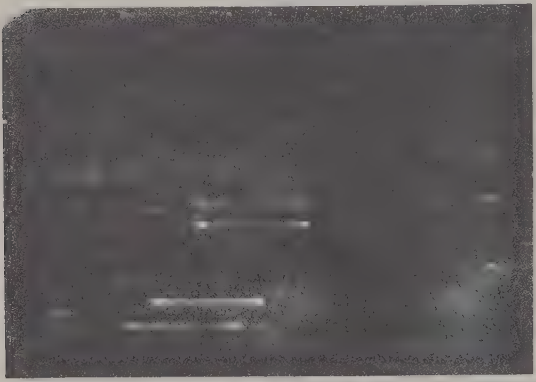

Abb. 5. Teilchenbewegung bei hartem Abschluß und der Frequenz 120 Hz.

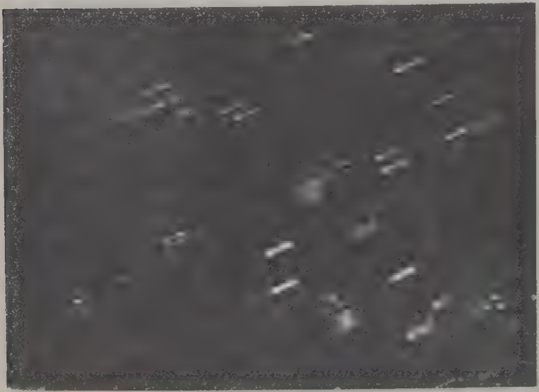

Abb. 6. Teilchenbewegung beim Rohrsystem mit Wattedämpfung für die Frequenz 260 Hz und die Stelle $z = 5{,}5$ cm.

5. Versuchsergebnisse

Es ist nun zu untersuchen, ob die experimentell ermittelten Größen der Schallfeldstruktur hinreichend gut mit den nach der MORSEschen Theorie bestimmten Werten übereinstimmen.

Auf Grund der im KUNDTschen Rohr ermittelten Impedanzen sind in den folgenden Abbildungen das Verhältnis der kleinen zur großen Ellipsenachse, sowie der Neigungswinkel der großen Ellipsenachse gegen die Rohrachse für die oben genannten drei akustischen Widerstände berechnet und durch ausgezogene Kurven dargestellt. Außerdem sind die experimentell ermittelten Werte durch kleine Kreise eingezeichnet.

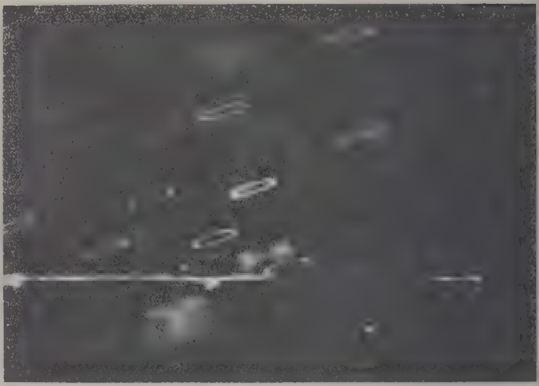

Abb. 7. Teilchenbewegung beim Abschluß mit dem Wellenwiderstand für die Frequenz 260 Hz und die Stelle $z = 5{,}5$ cm.

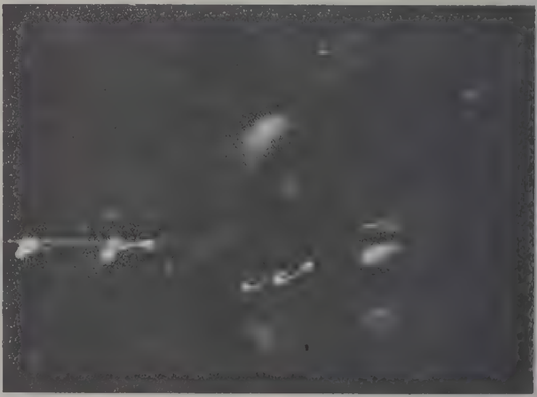

Abb. 8. Teilchenbewegung beim Abschluß mit dem Wellenwiderstand für die Frequenz 520 Hz und die Stelle $z = 5{,}5$ cm.

Die Abb. 9 und 10 zeigen das Achsenverhältnis und die Neigungswinkel für Glaswolle mit 30 cm Schichtdicke und einer Stopfdichte von 80 kg/m^3 vor hartem Abschluß (15 mm Eisenplatte) als Funktion der Frequenz für die Stellen $z = 2{,}5$ cm und $z = 5{,}5$ cm.

Glaswolle stellt im untersuchten Frequenzgebiet im wesentlichen einen Federungswiderstand dar. Solche Widerstände haben allgemein große elliptische Aufspaltung der Teilchenbewegung zur Folge. Dasselbe zeigt auch in Abb. 11 das Rohrsystem bei 520 Hz; bei dieser Frequenz besitzt das Rohr nach Abb. 4 fast rein „kapazitiven" Widerstand. Bei „induktiven“ Widerständen dagegen findet man nur geringe elliptische Aufspaltung, wie z.B. in Abb. 11 für das Rohrsystem bei 400 Hz.

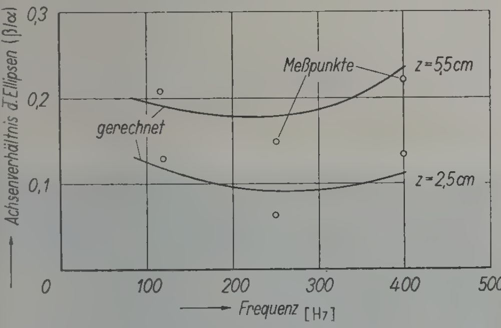

Abb. 9. Achsenverhältnis β/α der Ellipsen bei Glaswolle als Funktion der Frequenz.

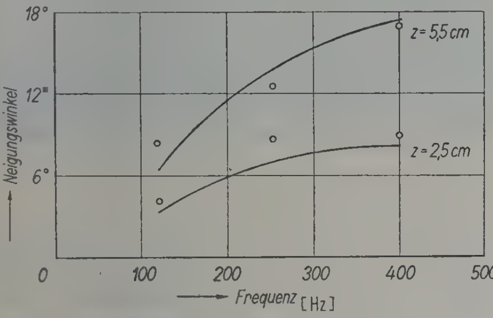

Abb. 10. Neigungswinkel δ der großen Ellipsenachse gegen die Rohrachse bei Glaswolle als Funktion der Frequenz.

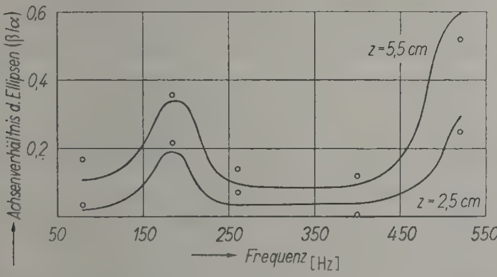

Abb. 11. Achsenverhältnis β/α beim Rohrsystem mit Wattedämpfung.

Dieses Verhalten ist auch verständlich z.B. durch Betrachtung des Phasenwinkels von $\overline{C}(H)$, also dem Verhältnis von Längswellenwiderstand zu Wandwiderstand an der Schluckstoffoberfläche ($C(H) = \varrho c/W$).

Der Längswellenwiderstand hat bemerkenswerterweise immer eine Blindkomponente in Form eines Massenwiderstandes. Bei Wandwiderständen mit einer Federungskomponente vergrößert sich daher der Phasenwinkel von $C(H)$ und damit auch die elliptische Aufspaltung, während bei Massenwiderständen der Phasenwinkel von $\overline{C}(H)$ abnimmt und dadurch eine Annäherung an die lineare Schwingung zustandekommt. Bei einem bestimmten Phasenwinkel des Wandwiderstandes kann man sogar ein reelles $C(H)$, d.h. eine geradlinige Schwingung erhalten.

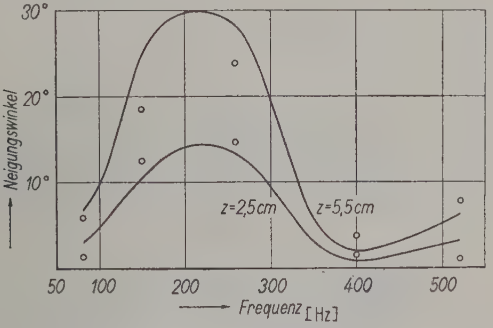

Abb. 12. Neigungswinkel δ beim Rohrsystem mit Wattedämpfung.

Das Rohrsystem und der Abschluß mit dem Wellenwiderstand sind zwei Beispiele für sehr verschiedenes Verhalten akustischer Widerstände (Abb. 11 und 14). Das eine Mal hängt die Impedanz stark von der Frequenz ab, während im anderen Fall weitgehende Frequenzunabhängigkeit vorhanden ist.

Das Rohrsystem hat bei der λ/4-Resonanz (etwa 200 Hz) einen sehr geringen Wirkwiderstand, während bei der λ/2-Resonanz (etwa 400 Hz) annähernd harter Abschluß erreicht wird. Dementsprechend ist auch der Verlauf des Neigungswinkels δ; bei der λ/4-Resonanz ist δ groß, bei der λ/2-Resonanz ist δ klein. Zwischen der λ/4- und λ/2-Resonanz ist der Widerstand „induktiv“, und deshalb muß das Achsenverhältnis der Ellipsen in Abb. 11 in diesem Bereich kleine Werte besitzen. Der Anstieg von β/α beginnt dann, wenn der akustische Widerstand reell oder „kapazitiv“ wird.

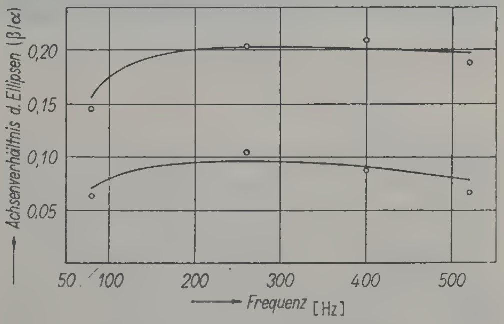

Abb. 13. Achsenverhältnis β/α beim Abschluß mit dem Wellenwiderstand (obere Kurve: $z = 5{,}5$ cm; untere Kurve: $z = 2{,}5$ cm).

Die Abb.13 und 14 bringen die Ergebnisse beim Abschluß mit dem Wellenwiderstand. Hier zeigt sich besonders gute Übereinstimmung der Messungen mit der Theorie.

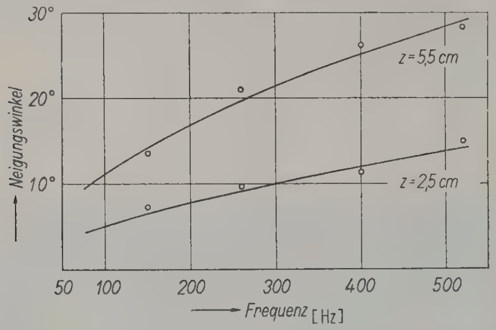

Abb. 14. Neigungswinkel δ beim Abschluß mit dem Wellenwiderstand.

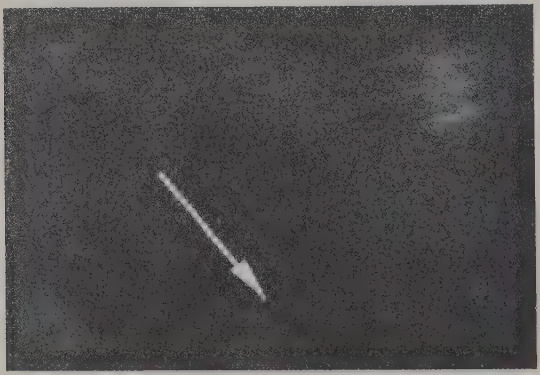

Abb. 15. Zum Rotationssinn der Teilchen; Glaswolle bei 400 Hz; die Pfeilrichtung gibt die überlagerte Geschwindigkeit an.

Abschließend sei noch eine Betrachtung über den Rotationssinn der Teilchen gemacht. Der Drehsinn hängt von der Phasenlage des Verhältnisses $C(z)$ ab, also an der Schluckstoffoberfläche gibt Gl.(8) den Drehsinn an. Der induktive Längswiderstand bedingt, daß man immer Teilchenumläufe im Uhrzeigersinn hat, sofern der Phasenwinkel des Wandwiderstandes nicht zu große, positive Werte besitzt.

Der Drehsinn des Teilchens läßt sich experimentell sehr einfach bestimmen[2]. Durch eine Gleichströmung vorgegebener Richtung wird dem schwingenden Teilchen eine zusätzliche Geschwindigkeit (Abb.15 und 16 in Pfeilrichtung) erteilt. Die entstehenden Spiralen lassen den Richtungssinn erkennen. Die Aufnahme wurde mit Glaswolle bei 400 Hz gemacht; dabei ist der Phasenwinkel von $C(H)$ etwa $+44^0$.

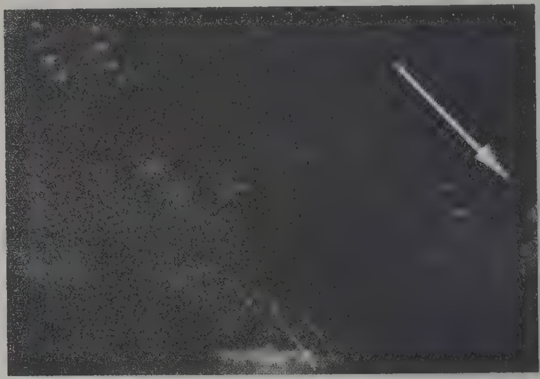

Abb. 16. wie Abb.15, aber für Rohrsystem mit Wattedämpfung bei 330 Hz.

Abb.16 gilt für das Rohrsystem bei 330 Hz. Nach Abb.4 hat das System hier einen hohen, induktiven Widerstand. Dieser große Phasenwinkel (63^0) des Wandwiderstandes vermag das Vorzeichen des Phasenwinkels von $C(H)$ zu ändern; er ist -31^0.

Der Drehsinn des Teilchens ist daher in Abb.15 im Uhrzeigersinn, während Abb.16 den entgegengesetzten Sinn zeigt.

(Eingegangen am 20. April 1951.)

Schrifttum

[1] v. BÉKÉSY, G., Z. techn. Phys. **14** [1933], 6.
[2] MEYER, E. und BUCHMANN, G., Akust. Z. **3** [1938], 139.
[3] JANOWSKY, W. und SPANDÖCK, F., Akust. Z. **2** [1937], 329.
[4] SIVIAN, L. J., J. acoust. Soc. Amer. **9** [1937], 135.
[5] CREMER, L., Akust. Z. **5** [1940], 57.
[6] MORSE, P. M., J. acoust. Soc. Amer. **11** [1939], 205.
[7] LIPPERT, W., Akust. Z. **6** [1941], 46.

---

[2] Vorschlag von K. TAMM.

PARAMETERS OF SOUND PROPAGATION IN GRANULAR ABSORBENT MATERIALS

by M. A. FERRERO and G. G. SACERDOTE
(Istituto Elettrotecnico Nazionale Galileo Ferraris, Torino, Italy)

Summary

From measurements of acoustical impedance of homogeneous absorbent materials made with the method of stationary waves, it is possible to determine the parameters of propagation. Measurements are made with two thicknesses of the material, one double of the other. The procedure followed for the calculation is indicated and some diagrams are proposed to obtain more easily the parameters of propagation. Examples are given of the method proposed and the parameters are calculated for small spherical leaden balls and sand of various sizes.

Sommaire

On peut déterminer les paramètres de propagation en partant des mesures de l'impédance acoustique des matériaux absorbants homogènes faites à l'aide de la méthode des ondes stationnaires. Des mesures ont été faites sur deux épaisseurs du matériau, l'une double de l'autre. Un procédé de calcul est donné et certains diagrammes sont proposés pour obtenir plus aisément les paramètres de propagation. Des exemples de la méthode proposée sont donnés et les paramètres sont calculés pour des petites balles sphériques de plomb et du sable de différentes grosseurs.

Zusammenfassung

Aus Messungen des akustischen Scheinwiderstandes homogener absorbierender Materialien mit Hilfe der Methode der stehenden Wellen kann man die Ausbreitungsparameter des Stoffes bestimmen. Die Messungen wurden bei zwei Schichtdicken des Materials durchgeführt, die sich wie 1:2 verhielten. Die Auswertungsmethode wird angegeben und es werden einige Diagramme vorgeschlagen, mit denen sich die Ausbreitungsparameter leicht berechnen lassen. Es werden einige Beispiele für die Anwendung der vorgeschlagenen Meßmethode gezeigt und die Ausbreitungskonstanten für kleine Bleikugeln und Sand verschiedener Größe berechnet.

1. Introduction

In the study of the absorbing properties of materials the determination of the parameters of sound propagation is very important, when the material can be considered of homogeneous structure. It is known that by electrical analogies we can compare the propagation of plane sound waves in absorbent materials to the propagation of an electrical perturbation in a homogeneous line with losses; we can then determine two kinds of parameters: the constant of propagation γ and the characteristic impedance Z_c, from which it is possible to deduce the definitive parameters: the equivalent resistance and reactance in series, the equivalent conductance and susceptance in parallel. The knowledge of these parameters is very important, because it allows a direct examination of the theories of sound propagation in granular materials. To deduce these parameters it is necessary first to determine the amplitude and phase of the propagation constant and of the characteristic impedance, which can be deduced from measurements of acoustical impedances.

2. Line of approach

We have examined the possibility of determining the characteristic parameters through the measurement of open circuit impedance for two different thicknesses of sample, or for two different lengths of the equivalent electrical line. In the method of measurement which has been adopted the material is fixed to a rigid piston, that is, to an infinite impedance: the measurement is then made with the load circuit open. It is advantageous to take the two thicknesses exactly in the ratio 2:1 because, then, the mathematics are easy to handle. A prerequisite for measurements of this kind is of course that the material under test is homogeneous indeed.

For a given thickness l of material (or length of equivalent electric line), the acoustical impedance Z measured at the surface of a sample backed by a rigid wall (infinite impedance) is

$$Z = Z_c \coth \gamma l.$$

For the length $2l$ we have:

$$Z' = Z_c \coth 2\gamma l.$$

Introducing the complex ratio: $u+\mathrm{j}v=Z/Z'=\coth\gamma l/\coth 2\gamma l$

$$u+\mathrm{j}v=\frac{1+\cosh 2\gamma l}{\cosh 2\gamma l};$$

whence: $[(u-1)+\mathrm{j}v]\cosh 2\gamma l=1$.

Putting $\gamma=\alpha+\mathrm{j}\beta$, α = attenuation constant, β = phase constant:

$$\cosh 2\alpha l\cos 2\beta l+\mathrm{j}\sinh 2\alpha l\sin 2\beta l=\frac{1}{(u-1)+\mathrm{j}v},$$

$$\cosh 2\alpha l\cos 2\beta l=\frac{u-1}{(u-1)^2+v^2},$$

$$\sinh 2\alpha l\sin 2\beta l=\frac{-v}{(u-1)^2+v^2}.$$

In the system of cartesian coordinates u and v, the lines αl constant and βl constant are given by:

$$\frac{(u-1)^2}{\cos^2 2\beta l}-\frac{v^2}{\sin^2 2\beta l}=[(u-1)^2+v^2]^2,$$

$$\frac{(u-1)^2}{\cosh^2 2\alpha l}+\frac{v^2}{\sinh^2 2\alpha l}=[(u-1)^2+v^2]^2.$$

Shifting the centre of the coordinates to the point $u=1$, $v=0$, and transforming into polar coordinates (ρ, Θ) we obtain:

$$\rho=\frac{\sqrt{2}}{\sin 4\beta l}\cdot\sqrt{\cos 2\Theta-\cos 4\beta l},$$

$$\rho=\frac{\sqrt{2}}{\sinh 4\alpha l}\cdot\sqrt{\cosh 4\alpha l-\cos 2\Theta}.$$

The curves αl constant and βl constant in the complex u, v plane are traced in Fig. 1: all curves of the set αl intersect those of the set βl orthogonally. The lines of constant βl pass through the point $u=1$, $v=0$; they have the form of a lemniscate, which for $\beta l=0$ is reduced to the segment of the abscissa between $u=0$ and $u=2$; for $\beta l=\pi/4$ we have the straight line $u=1$.

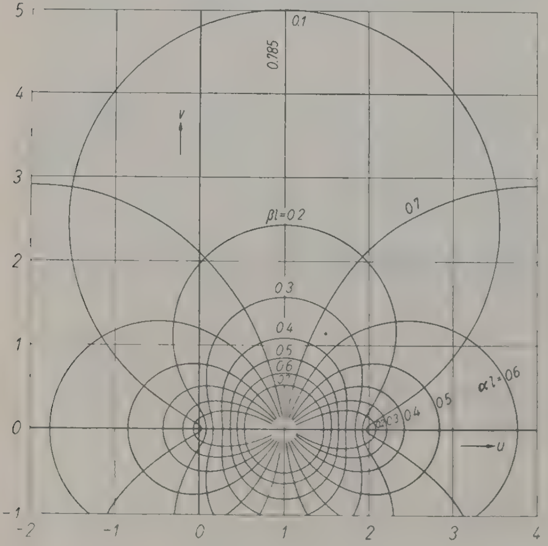

Fig. 1. Diagram of the lines αl constant and βl constant.

The lines αl constant for high values of αl tend to become circles with centre at the point (1,0) and radius $\sqrt{2}\cdot\exp(-2\alpha l)$.

From the measurement of the impedance for the lengths l and $2l$ the components of the quantity $u+\mathrm{j}v=Z/Z'$ can be deduced graphically or analytically; from the diagram of Fig. 1 the values of αl and βl are found, from which α and β. We note that this operation can be performed for different lengths of material, one double of the other; the corresponding representative points in the u, v plane vary with l: the representative line of the quantity $u+\mathrm{j}v$ is a spiral that starts from the point $u=2$, $v=0$, and revolves round the apex $u=1$, $v=0$.

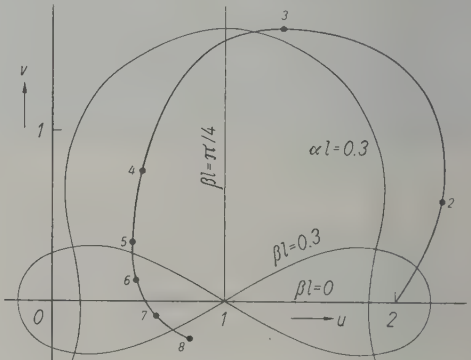

Fig. 2. Values of the quantity $u+\mathrm{j}v$ as function of l.

The possibility of tracing this spiral for many couples of values of lengths one double of the other permits a judgement on the degree of approximation that can be reached. In Fig. 2 one of these spirals is traced, obtained from impedance measurements for lengths of material between 2 and 16 cm. The values of α and β obtained with this method present differences of 1 to 2%: the possibility of measurements on different couples of length one double of the other permits a control of the results, which cannot be obtained when the measurements are made only with closed and open circuits on one length of material.

Once the propagation constant γ is found, we obtain: $Z_c=Z\tanh\gamma l$. The calculation of Z_c is easily made graphically. From the general theories of long lines we have:

$$Z_c=\sqrt{z/y},\ \gamma=\sqrt{zy}$$

(z is the distributed impedance in series and y is the distributed admittance to the earth); then:

$$z=Z_c\cdot\gamma;\quad y=\gamma/Z_c.$$

The impedance z has a real component which is the equivalent resistance per unit of length, and an imaginary component, which after dividing by $j\omega$ gives the equivalent inductance in series; from the admittance the values of the equivalent conductance and capacitance can be deduced.

3. Measurements

With the method described in section 2 we have made a series of measurements on materials with granular structure; this research has been made for studying a material having a well-defined structure, so that the measurements can be repeated with different methods and give interesting comparisons, since with the simple structure of the material under examination, it is possible to compare the experimental results with the theoretical data.

The material first chosen consisted of small spherical leaden balls of the following three sizes:

leaden balls N. 1	diameter	3.70 mm
″ ″ ″ 2	″	2.55 ″
″ ″ ″ 3	″	1.95 ″

Then we have used sand of various sizes:

sand N. 1	diameter	2—2.5 mm
″ ″ 2	″	1—2 ″
″ ″ 3	″	0.5—1 ″
″ ″ 4	″	0.33—0.50 ″
″ ″ 5	″	0.25—0.33 ″

The measurements on these granular materials are especially advantageous, because the determination can be made in a tube in stationary waves, and in this case the great importance of the conditions of the support of the material at the bottom and at the edges is well known. In our measurements the experimental tube is set vertical and the leaden balls or the sands were poured into a metallic cylinder fixed to the movable piston, just as a liquid,

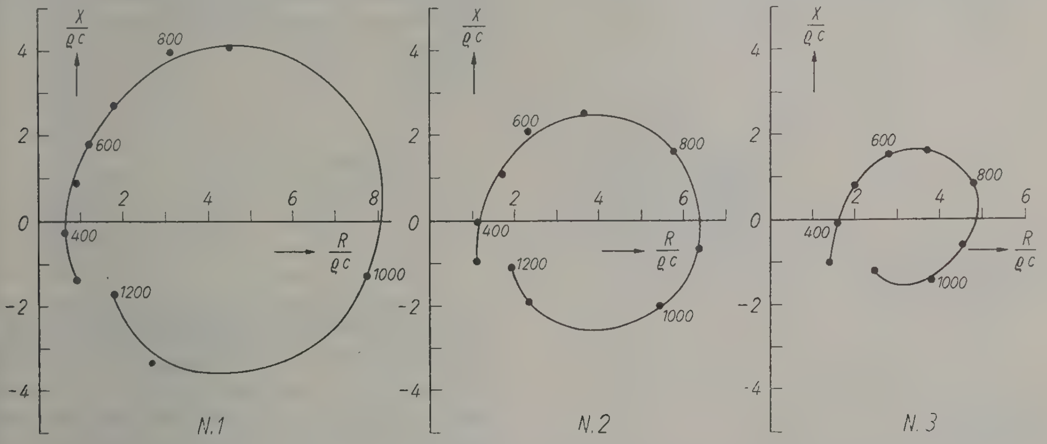

Fig. 3. Vectorial diagram of the acoustical impedance for leaden balls of various sizes, at variable frequency and constant length (14 cm).

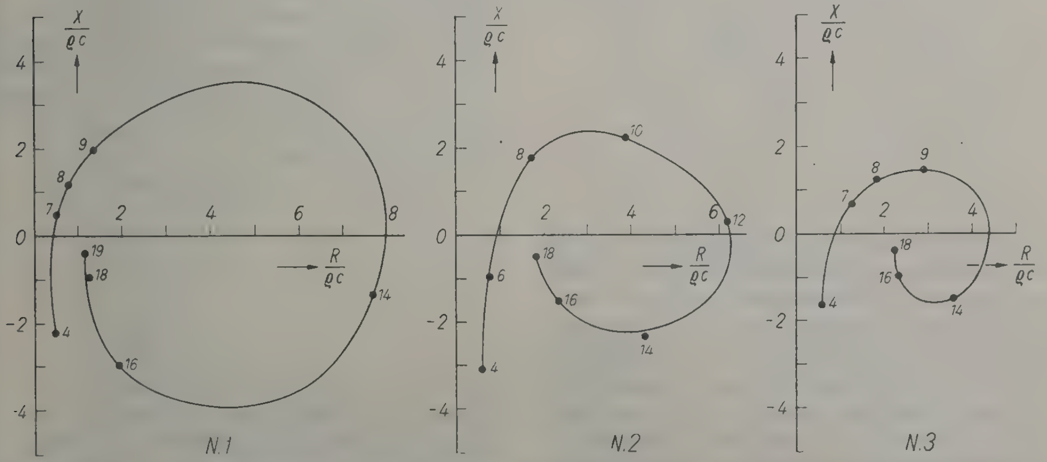

Fig. 4. Vectorial diagram of the acoustical impedance for leaden balls of various sizes, at variable length and constant frequency (1000 Hz).

so that the uncertainties caused by the support conditions were eliminated. Moreover it is possible to vary continuously the length of the material under examination: this is very important for the method of measurement chosen, which is based on the comparison of different determinations made on material of various lengths.

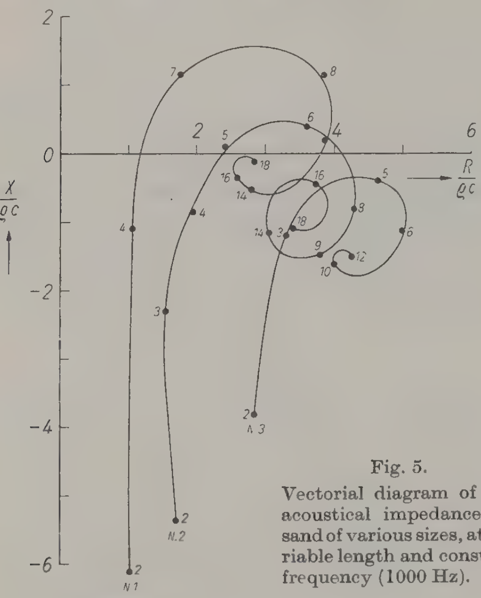

Fig. 5. Vectorial diagram of the acoustical impedance for sand of various sizes, at variable length and constant frequency (1000 Hz).

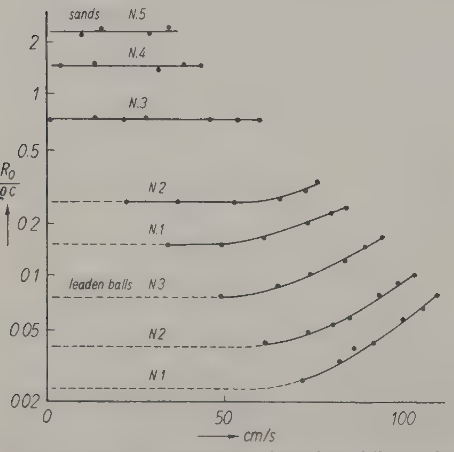

Fig. 6. Specific flow resistance as function of flow velocity.

And finally it is possible to repeat the measurements under the same conditions at great intervals of time and with different measuring apparatus. When using leaden balls which have a well-defined structure the measurements were repeated with considerable regularity, however for the sand especially of small sizes some uncertain factors caused by variations in structure and by the state of humidity of the sand interfere.

Measurements of impedance were made with the technique indicated by **Beranek** [1], for different thicknesses of material. The absorption of the tube as functions of the length and the frequency has been found to be analogous to that reported by **Beranek** in the note cited.

Figures 3, 4 and 5 report some of the experimental results. We must point out that the leaden balls have a geometrical form, quite regular and of constant diameter, while in the case of the sand the small grains are different in form and size, and some impalpable dust is always present.

4. Discussion

In order to coordinate the experimental results with theoretical data, it is necessary to determine directly the porosity of the material, i.e., the ratio between the volume of air contained in the material and the whole volume of the material itself. Determinations of the porosity have given the following results:

leaden balls N. 1	porosity	0.39
″ ″ ″ 2	″	0.39
″ ″ ″ 3	″	0.38
sand ″ 1	″	0.41
″ ″ 2	″	0.40
″ ″ 3	″	0.37
″ ″ 4	″	0.40
″ ″ 5	″	0.47

By theoretical considerations on a space being filled with spheres of the same radius, it results that the maximum filling up of the space gives a porosity 0.26; with other distributions of the spheres we obtain the porosities 0.48 and 0.66. Experimentally we have found the intermediate value 0.39, independent of the diameters of the grains.

Then we have measured the flow resistance (the ratio between the pressure fall through a sample of material of given length and section, and the velocity of the air particles flowing through the sample itself). If R_0 is the specific flow resistance $(L^{-3} M T^{-1})$ we have the following results:

leaden balls N. 1	$R_0/\rho c$	= 0.024	cm⁻¹
″ ″ ″ 2	″	= 0.041	″
″ ″ ″ 3	″	= 0.075	″
″ ″ 1	″	= 0.15	″
″ ″ 2	″	= 0.27	″
″ ″ 3	″	= 0.75	″
″ ″ 4	″	= 1.50	″
″ ″ 5	″	= 2.35	″

ρc being the specific acoustic impedance of air.

The value of the flow resistance is a function of the flow velocity [2]: this is shown in the curves of Fig. 6. We observe that the limiting resistance R_0

and the diameter ***d*** of the grains are related by the equations experimentally deduced:

$R_0\, d^{1.30}$ = constant for sands,
$R_0\, d^{1.80}$ = constant for leaden balls.

The curves of Fig. 7 and 8 show the values of the real and imaginary parts (α and β) of the propagation constant for the leaden balls and the sands.

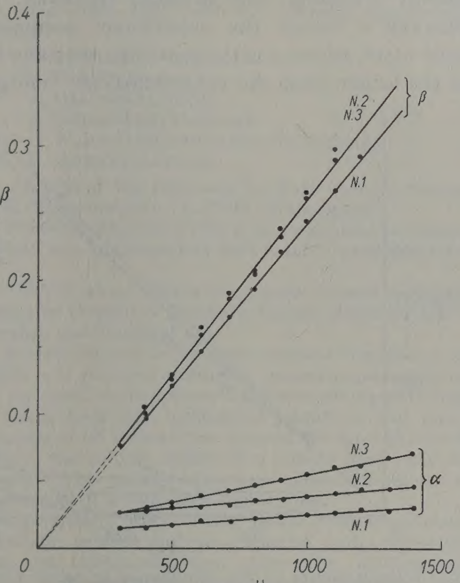

Fig. 7. Propagation parameters as function of the frequency for leaden balls of various sizes.

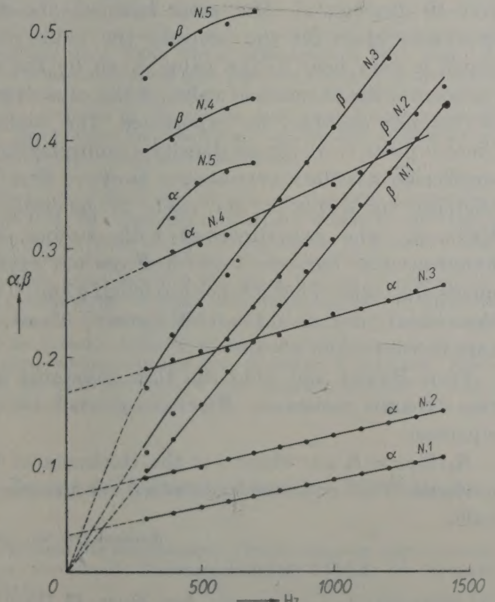

Fig. 8. Propagation parameters as function of the frequency for sands of various sizes.

The characteristic impedance deduced from these data is reported in Fig. 9, and then in Fig. 10, 11, 12 and 13 the primary parameters: the equivalent resistance and inductance in series, the equivalent capacitance and conductance in series.

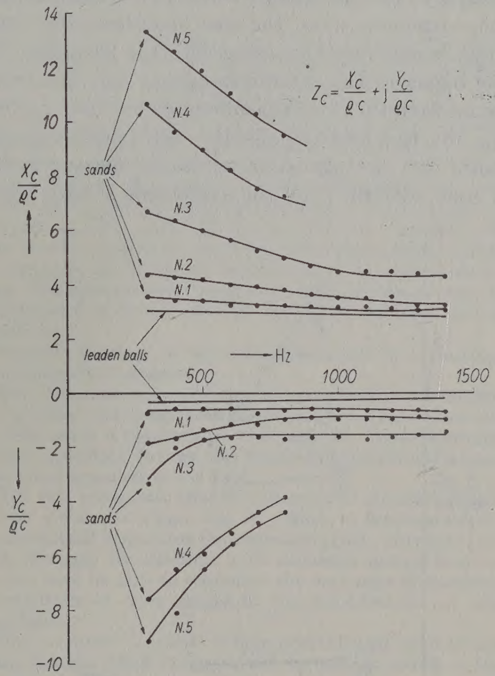

Fig. 9. Real and imaginary components of characteristic impedance as function of frequency, for leaden balls and sands.

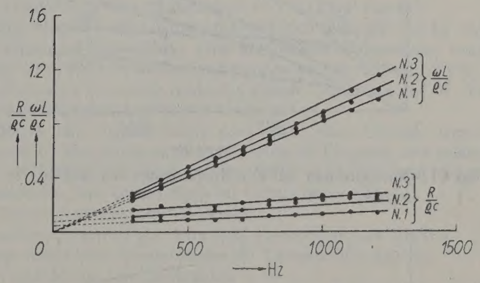

Fig. 10. Components of the impedance in series for leaden balls.

From the data reported we can observe:

a) in the case of small leaden balls the resistance increases slightly with the frequency, whereas the capacitance, the inductance and the conductance are constant: moreover the inductance and the capacitance do not vary when we change the size of the grains.

b) in the case of the sands the capacitance becomes constant and varies very little with the size of the grains; its value is near that of the leaden balls. The conductance is very low and of the same order as in the case of the leaden balls. On the contrary the inductance and the resistance are more irregular when the size decreases: the resistance is regularly increasing with the frequency for the bigger grains. At the frequency zero the value found from the flow measurements has been reported: for the leaden balls the agreement between static flow and dynamic resistance measurements is good. For the sand the agreement is good when the grains are not to small: for the small grains the flow resistance is much smaller than it should be by extrapolation towards zero of the values found through acoustic impedance measurements. The values of the conductance are generally very low.

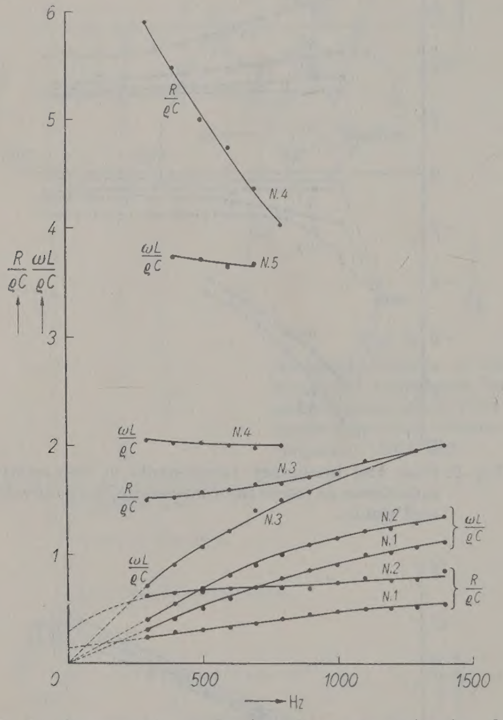

Fig. 11. Components of the impedance in series for the sands.

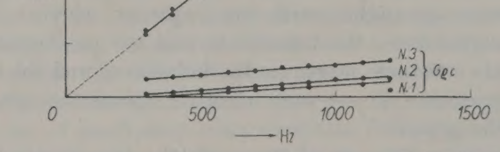

Fig. 12. Components of the admittance in parallel for leaden balls.

The theory of the impedance of granular materials has been developed by **Morse**, **Bolt** and **Brown**, **Zwikker** and **Kosten**, **Beranek**. From **Beranek**'s theory the capacitance assumes the value $\pi/\rho c^2$, where π is the porosity: we have found for the leaden balls the value $0.304 \cdot 10^{-6}$ cm^{2}g^{-1}s^2.

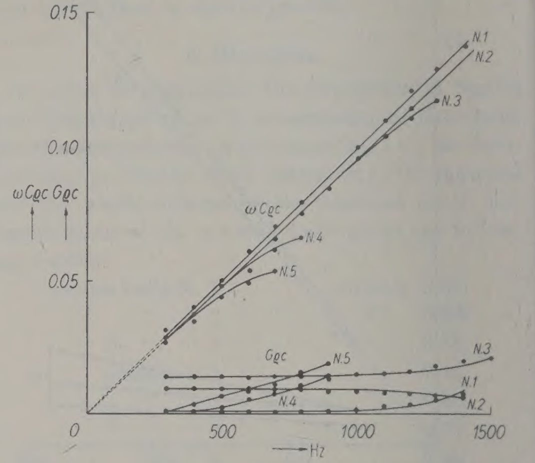

Fig. 13. Components of the admittance in parallel for the sands.

The value for air in adiabatic propagation is $0.71 \cdot 10^{-6}$ cm^{2}g^{-1}s^2. The ratio between the two quantities gives for the porosity the value 0.42, which is very near to the value given by the experiments: the theoretical value of the capacitance is therefore justified by experience. The conductance is given from the air density ρ multiplied by a coefficient s, called structure factor, first introduced by **Zwikker**: its value is generally 3; **Beranek**, who experimented with meshes, has found a value between 2 and 3. From our experiments the value of inductance is 0.00522 g cm^{-3}: the theoretical value should be 0.0012 g cm^{-3}. The structure factor is then $s = 4.3$.

From **Brown** and **Bolt** the flow resistance and the dynamic resistance $R/\rho c$ are related by the equation:

$R_0 l / 3 \rho c = R / \rho c$, where l is the thickness of the material. This equation is satisfied for the leaden balls.

(Received 29th May, 1951.)

References

[1] **Beranek**, L. L., J. acoust. Soc. Amer. **12** [1940], 3.
[2] **Brown**, R. L. and **Bolt**, R. H., J. acoust. Soc. Amer. **13** [1942], 337.

Report on the first meeting of the International Commission on Acoustics

The International Commission on Acoustics (ICA) was created at the General Assembly of the International Union of Pure and Applied Physics (IUPAP) held in Copenhagen 10th—13th July 1951. The ICA was designated a Special Commission of the IUPAP[1].

This Commission held its first meeting in London, September 11th—14th 1951, with the following members in attendance:

R. H. BOLT, President, U.S.A.
F. CANAC, France
A. GIACOMINI, Italy
F. INGERSLEV, Denmark
C. W. KOSTEN, Secretary, Netherlands
E. MEYER, Germany.

The address of the Secretary is: Lab. voor Technische Physica, Mijnbouwplein 11, Delft, Netherlands.

The President suggested that a vice-president be chosen. Mr. CANAC was nominated as such and accepted this function.

The IUPAP comes within the general framework of the International Council of Scientific Unions, under UNESCO sponsorship and financial aid.

The general purpose of the International Commission on Acoustics is to promote and foster international collaboration in pure and applied acoustics. The contemporary field of acoustics deals with mechanical vibrations and waves in all media at all frequencies. Beyond the normal bounds of physics, the subject matter of acoustics inherently encompasses a wide variety of topics that are also related to other domains of science and engineering.

More specifically, the currently active branches of acoustics include: general physical acoustics, audio communications and electro-acoustics, ultrasonics, architectural acoustics, industrial noise control, musical acoustics, physiological and psychological acoustics, industrial processing and testing by sound, and medical and biological applications of acoustics.

There are at least seven[2] societies or groups devoted specifically to acoustics, with a combined membership of something over 2000. These organisations have more or less official connections with national societies or institutes of physics. In addition there are many scientific and engineering societies in other fields, such as electrical engineering, psychology and medicine, which are interested in certain special branches of acoustics.

This diversity of subject matter and activities was a major topic of discussion at this meeting. The programme of the ICA, its scope and limitations, should be developed rationally in terms of the present status of acoustics. Duplication of effort should be avoided, but there appears to be certain areas in which the dissemination of information and the exchange of views could be facilitated. In time the ICA should probably become an Affiliated Commission with an expanded organizational structure, capable of serving more adequately the diverse fields of acoustics. However, the members believe that expansion should proceed conservatively, and that for two years or so a suitable programme can be developed within the confines of a small Special Commission.

For its first programme item, the ICA will establish immediately an international clearing house for schedules of major meetings in acoustics. The Secretariat of the ICA invites herewith the establishment of regular communication with the secretaries of all existing societies in acoustics. Through these channels the ICA will attempt to maintain a master calender of all major meetings that have been planned or that are being contemplated in any country. It would be helpful for this information to be received as early as possible after any dates are fixed. The ICA will thus be able to answer enquiries regarding dates, locations and general nature of the programme of any future meetings. This information would be submitted twice a year to the Journal of the Acoustical Society of America and to Acustica.

Another function of the Commission will be to arrange international congresses.

The Commission is exploring the possibility of arranging an international Congress in the Netherlands in the summer of 1953, with a programme that may be oriented around electro-acoustics. It may also be possible to arrange a more restricted symposium for 1952.

The ICA recognizes that the question of standardization is not within its scope, but is, rather, a function of the International Standards Organization (ISO). However, the ICA, through its relations with acoustics groups and societies, may be able to stimulate the exchange of technical information at early stages in the consideration of new standards.

The calender of events is being established at once and plans for the 1953 Congress will be announced in a few months. Other activities will be considered by correspondence during the year and the Commission will meet again in the summer of 1952.

The Secretary.

---

[1] Article 6 of the Statutes of the IUPAP reads:

„The General Assembly and, subject to approval by the next General Assembly, the Executive Committee may decide to create Commissions proper to the Union of Physics and also to participate in Joint Commissions of the Union of Physics and other Unions.

Among the Commission proper to the Unions some, devoted to the more extensive fields of Physics, are called Affiliated Commissions; others, with more limited terms of reference, are called Special Commissions''.

[2] Acoustical Society of America,
Acoustics Group of the Physical Society of London,
Groupement des Acousticiens de Langue Française,
Geluidstichting (Netherlands),
Gruppo d'acustica della Società italiana di fisica,
Swedish Acoustical Society,
Fachgruppe für Akustik im Verbande der Deutschen Physikalischen Gesellschaften.

We should be glad to receive information on any other acoustics groups that may be in existence.

Tagung des Verbandes Deutscher Physikalischer Gesellschaften vom 19. bis 23. 9. 1951 in Karlsruhe

Anläßlich der diesjährigen Physikertagung wurden auch einige interessante Vorträge aus dem Gebiete der Akustik gehalten.

E. SCHREUER, Karlsruhe, berichtete über „GOUGH-JOULE-Effekt und thermische Schwingungsdämpfung''. Im Gegensatz zu den meisten Stoffen, z. B. Metallen, erwärmt sich Gummi, wenn er dilatiert wird (GOUGH-JOULE-Effekt); sein Volumen verkleinert sich dabei. Die auftretende Kompressionswärme kann als Umwandlungswärme erklärt werden, denn die Gummimoleküle nehmen unter Zug eine geordnete Lage ein. Der Proportionalitätsfaktor zwischen

Volumenänderung bzw. adiabatischer Druckänderung und Temperaturänderung ist eine unabhängige Stoffkonstante, welche sich für verschiedene Gummisorten aus den Daten der Mischungskomponenten berechnen läßt. Der Übergang in den ungeordneten Ruhezustand der Gummimoleküle ist als Ausgleichsvorgang mit einer Relaxationszeit behaftet und bewirkt eine thermische Schwingungsdämpfung, die sich unter einfachen Annahmen berechnen läßt.

W. GÜTTNER, Erlangen, referierte „Über Ultraschallabbildungen am menschlichen Schädel" und wies an Hand von umfangreichen Meßergebnissen nach, daß Hirntumor-Diagnoseverfahren mittels akustischer Abbildung von Hirnkammern, welche notwendigerweise Schallschwächungs-Meßverfahren sein müssen, bei Verwendung einer Schallfrequenz um 2 MHz keine brauchbaren Ergebnisse liefern können, weil der Einfluß der Knochenstruktur des Schädels die akustischen Effekte von Hirnkammern überdeckt.

A. LUTSCH, Erlangen, sprach über „Eine einfache Methode zur Bestimmung der elastischen Konstanten mit Hilfe von Ultraschallimpulsen". Ein an der Stirnfläche einer stabförmigen Probe von mehreren Wellenlängen Durchmesser erzeugter Ultraschallimpuls trifft wegen der Divergenz des Schallbündels nicht nur die gegenüberliegende Stirnfläche, wo er reflektiert wird, sondern streifend auch die Längswände, an denen er in Longitudinal- und Transversalwelle aufspaltet. Die Transversalwelle durchquert den Stab und erzeugt bei weiteren Reflexionen an den Längswänden Longitudinalkomponenten, die nach Reflexion am Stabende, je nach der Zahl der Stabdurchquerungen, um Vielfache einer bestimmten Zeitdifferenz später am Sendeort wieder eintreffen als der erste Impuls. Aus der Zeitdifferenz kann man bei bekannter Materialdichte alle elastischen Konstanten des Materials bestimmen. Die Messungen wurden mit einer Apparatur ausgeführt, die ähnlich wie das FIRESTONEsche Reflektoskop zur Auffindung von Materialfehlern entwickelt wurde. Die Diskussion ergab, daß H. SCHARDIN ähnliche Aufspaltung von reflektierten Impulsen in geraden und gebogenen stabförmigen Proben beobachtete.

H. OERTEL, Weil a. Rh., sprach über „Knallwellenoszillographie mittels einer Koronasonde". Die Koronasonde besteht aus zwei kleinen Platinkugeln (0,3 mm ∅) in einem Abstand von etwa 2 mm, an die eine Spannung von 5 ... 10 kV angelegt wird. Die sich ausbildende Korona ist druckempfindlich, was man im Druckkessel in Abhängigkeit von der Dichte feststellen kann. Das Gerät ist praktisch trägheits- und reflexionsfrei; allerdings ist die Geräuschspannung sehr hoch, so daß nur Knallwellen oder dergleichen gemessen werden können. Eine Reihe von Messungen (Ausbreitung von Knallwellen, Laufzeit-, Beugungs- und Reflexionsuntersuchungen) belegen die Brauchbarkeit des Verfahrens; es zeigt, wie erwähnt, den Schalldruck an im Gegensatz zum Kathodophon (durch Thermoionen ionisierte Luftstrecke), das auf die Schallelongation anspricht.

K. Tamm.

Bookreviews

L. E. KINSLER and A. R. FREY, Fundamentals of acoustics. New York, John Wiley; London, Chapman and Hall; 1950, 516 pages, 14×21 cm², 165 fig. Price $ 6,00.

A good title for a good book. The fundamentals are thoroughly described in the first 9 chapters, meant for a one-semester course in theoretical acoustics. These chapters deal with vibrations, strings, bars, membranes, plates, plane and spherical waves in air, resonators, filters and absorption. The following 7 chapters are independent of each other and deal with the main applications and practical problems, e. g. loudspeakers, microphones, psycho-acoustics, architectural acoustics, underwater acoustics and ultrasonics. The whole book could serve, according to the writers, for a one-year's course in theoretical and applied acoustics. For Dutch circumstances this applies indeed very well. The book fits in almost ideally after two years study at a university. The suitability for educational purposes is greatly enhanced by the addition of instructive problems at the end of every chapter.

The introduction of the velocity potential is made rather mysteriously. Fortunately it is only seldom used. The units used are combined CGS (mechanics) and practical (electricity), which is acceptable, although not ideal (MKS seems more attractive as a coherent system).

The book is not meant as a reference work. It may greatly be recommanded as a thorough introduction to theoretical and applied acoustics for those having some feeling for electrotechnics. Complex notation is used throughout the book.

C. W. Kosten, Delft.

W. MEYER-EPPLER, Elektrische Klangerzeugung. F. Dümmlers Verlag, Bonn 1949, 140 Seiten, 122 Abb., DIN A 5, DM 10,80.

Zwei große Gebiete werden in neuerer Zeit wesentlich durch die elektrische Klangerzeugung beeinflußt: die Musik, oder genauer die Tonkunst, und die synthetische Sprache. Die elektrische Klangerzeugung bietet auf beiden Gebieten sowohl dem Akustiker als auch dem Phonetiker neben der bekannten Analyse nun auch die Möglichkeit zur Klangsynthese. Dem Musiker werden neuartige Klänge und Instrumente zur Verfügung gestellt, dem Techniker wird die Möglichkeit gegeben, die über weite Entfernungen übertragenen Elemente einer Nachricht wieder in Sprache zu verwandeln.

Das vielseitige Interesse für diese Gebiete hat zu einer Fülle von Arbeiten und Geräten geführt, so daß die Absicht des Verfassers, in dem vorliegenden Buche eine möglichst umfassende Darstellung des ganzen Gebietes der elektrischen Klangerzeugung ohne zu tiefes Eingehen auf die rein technische Seite zu geben, nur begrüßt werden kann.

Ausgehend von den akustischen Grundbegriffen und den Eigenschaften des Gehörs werden im 1. Teil des Buches die Klangempfindungen (Lautstärke, Tonhöhe, Schwebungen, Geräusche, Klangfarbe, Einschwingvorgänge) untersucht. Der 2. Teil behandelt die allgemeinen Grundlagen der elektrischen Klangerzeugung, die Generatoren, die Spielmechanik und die elektrischen und elektroakustischen Hilfsmittel zur Beeinflussung der Klangeigenschaften und zur Abstrahlung des Schalles. Im 3. Teil werden schließlich die einzelnen Geräte für elektrische Klangerzeugung, d. h. die elektronischen Musikinstrumente (Geräte mit schwingenden Saiten, Röhrengeneratoren, Glimmröhrengeneratoren, Transponierungsgeneratoren, rotierenden Profilscheiben) und die Geräte für die synthetische Sprache (Voder, Vocoder) in einzelnen Beispielen besprochen. Dabei werden nur wirklich ausgeführte Geräte berücksichtigt, nicht aber die umfangreiche Patentliteratur; technische Einzelheiten werden in dem begrenzten Rahmen des Buches nicht behandelt. Eine besonders willkommene Ergänzung des dargestellten Stoffes ist das umfangreiche Literaturverzeichnis.

Die gute Gliederung des Buches, die Vermeidung langer theoretischer Ableitungen, die große Anzahl von Skizzen, Tabellen und Abbildungen machen das Buch in gleicher Weise für den Studenten wie für den Praktiker und für den Musiker zu einem wertvollen Studien- und Nachschlagewerk.

K. Tamm.